MONITORING CHANGES OF CLOUDS

WILLIAM B. ROSSOW
NASA Goddard Institute for Space Studies, New York, NY 10025, U.S.A.
and
BRIAN CAIRNS
Columbia University, New York, NY 10027, U.S.A.

Abstract. An analysis of the spatial and temporal scales of cloud variability and their coupling provided by the results from existing cloud observing systems allows us to reach the following conclusions about the necessary attributes of a cloud monitoring system. (1) Complete global coverage with uniform density is necessary to obtain an unbiased estimate of cloud change and an estimate of the reliability with which that change can be determined. (2) A spatial sampling interval of less than 50 km is required so that cloud cover distributions will generally be homogeneous, or statistically homogeneous, within a sample. (3) A sampling frequency of at least six times a day ensures not only that the diurnal and semi-diurnal cycles are not aliased into long term mean values, but also that changes in them can be monitored. (4) Since estimated climate changes are only evident on a decadal time-scale, unless cloud monitoring is continuous with a record length greater than 10 years and has very high precision ($\approx$ 1%) instrument calibration with overlapping observations between each pair of instruments, it will not be possible either to detect or to diagnose the effects of cloud changes on the climate.

1. Introduction

Proper monitoring of changes in clouds that can feedback on climate changes must account for the large variety of cloud characteristics and their complex space-time variations. Because clouds on Earth are formed by condensation of water vapor, their variations are under control of and exhibit similar variations as the atmospheric motions (e.g., Rossow, 1978). The key characteristics of atmospheric motions are that they vary over a large range of space-time scales and that variations at particular space-time scales are coupled. Thus, clouds vary on time scales from $\sim$ 10 min to (at least) $\sim$ 10 yr and on space scales from $\sim$ 30 m to $\approx$ 40,000 km; but the smallest/largest time scales are associated with the smallest/largest space scales (Figure 1). Once we know something about the spectrum of cloud variations with scale, we can design an observing system to monitor cloud changes that is not a 'brute force' approach that simply resolves the smallest scales and covers the largest scales. In fact, the coupling of space-time scales makes this approach very impractical, requiring global images at 5 min intervals with a spatial resolution of 15 m. However, we need to do more than merely detect change; rather we need to be able to evaluate the effects of such changes on the climate, which requires more detailed observations than needed for change detection.

The shapes of the distributions of cloud properties are not even approximately Gaussian (Rossow and Schiffer, 1991). Surface and satellite determinations of cloud areal coverage both show that the distribution of this quantity is bi-modal

Climatic Change **31:** 305–347, 1995.

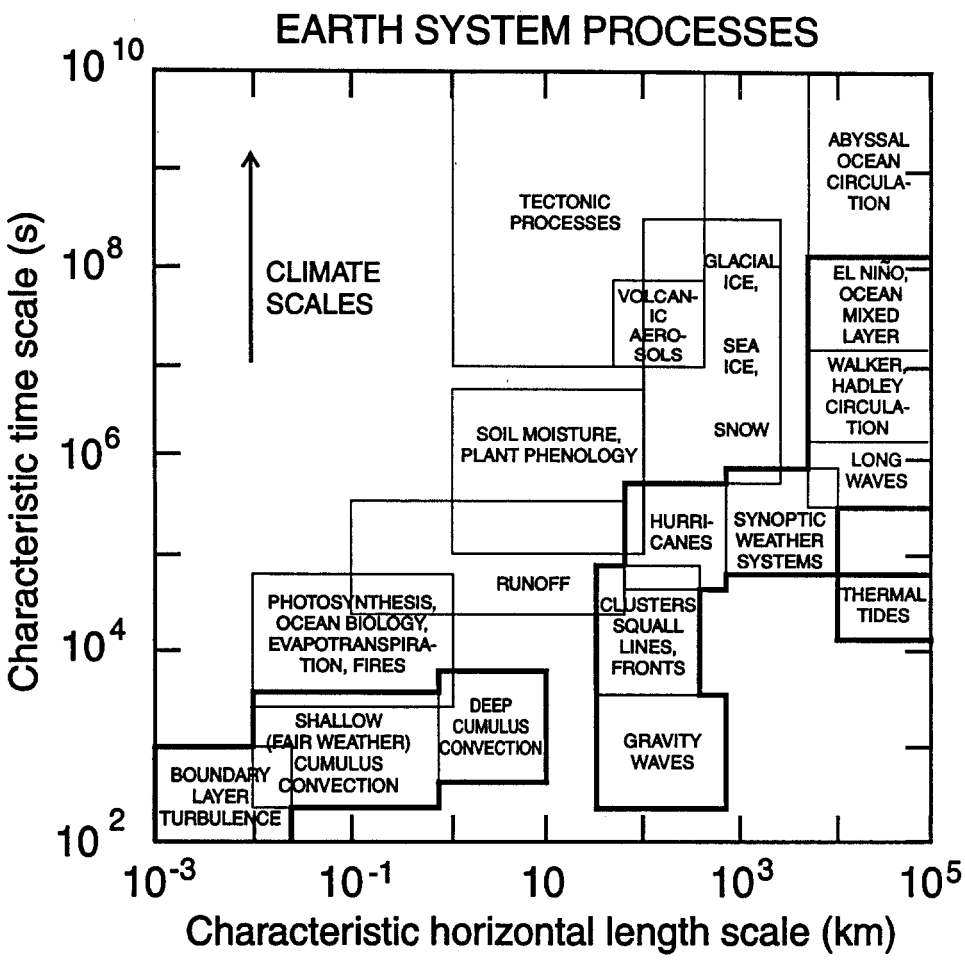

Fig. 1. Schematic of spatial and temporal scales associated with Earth system processes.

at smaller ($\lesssim$ 200 km) spatial scales (Figure 2). The optical thickness (or water content) distribution is monomodal, but very asymmetric with the largest values occurring very rarely and being more than 40 times larger than the most frequently occurring values (Figure 3a). When plotted on a scale that is linear in the radiative effect of cloud optical thickness (Figure 3b), the distribution is very broad but still shows a preponderance of optically thin clouds. The distribution of cloud top pressures viewed from satellites (Figure 4) is almost uniform over the range from 300 to 800 mb with a weak concentration at higher values (more low-level clouds). Obscuration of lower level clouds by higher clouds reduces the concentration at lower levels somewhat. There is also a small secondary concentration near the tropopause (100 mb) but the reality of this feature is uncertain (Liao *et al*, 1995a, b).

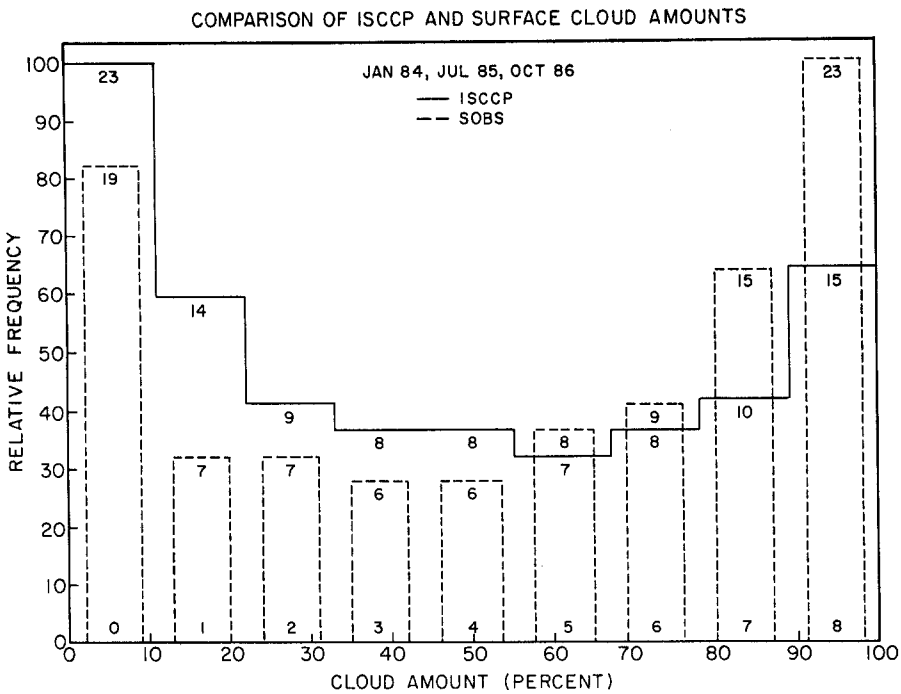

Fig. 2. Frequency distribution of cloud amounts in each octa (12.5%) over land from individual surface observations (dashed line) and the ISCCP analysis (solid line) for January 1984, July 1985 and October 1986. The ISCCP analysis is for areas about 280 km across and the surface observations represent areas about 50 km across. Fractions of total population in percent in each cloud amount interval are indicated by numbers near the top of each bar.

These one dimensional distributions (Figures 3 and 4) are misleading because the variations of these two basic cloud properties are correlated, producing more complicated structures that can be described in terms of the occurrence of different cloud types (Rossow and Schiffer, 1991). Figure 5 contrasts the distributions of cloud properties in the tropics, subtropical oceans and midlatitudes. Since the effects of clouds on the planetary radiation budget and hydrological cycle are strongly non-linear functions of these cloud properties, the dominant cloud types in the radiation budget are not the dominant clouds in the hydrological cycle. The most frequently occurring clouds are lower-level and lower optical thickness, so that they dominate the radiation budget on average (Rossow and Zhang, 1995); whereas the key cloud types in the hydrological cycle are the relatively rare precipitating systems characterized by high optical thicknesses and high top heights (Lin and Rossow, 1994). Moreover, the relation of cloud properties to atmospheric motions is more likely to involve variations of cloud types expressed as correlated changes in several cloud properties (cf. Lau and Crane, 1995). Thus, cloud changes cannot be adequately described by an average and standard deviation of the cloud properties, determined separately; rather cloud changes must be described by **correlated**

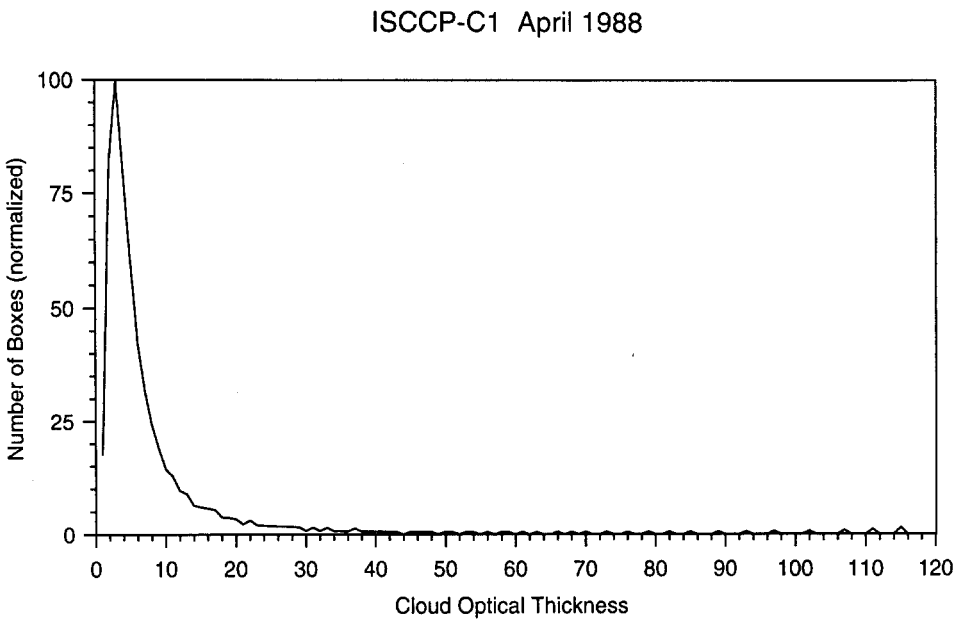

Fig. 3a.

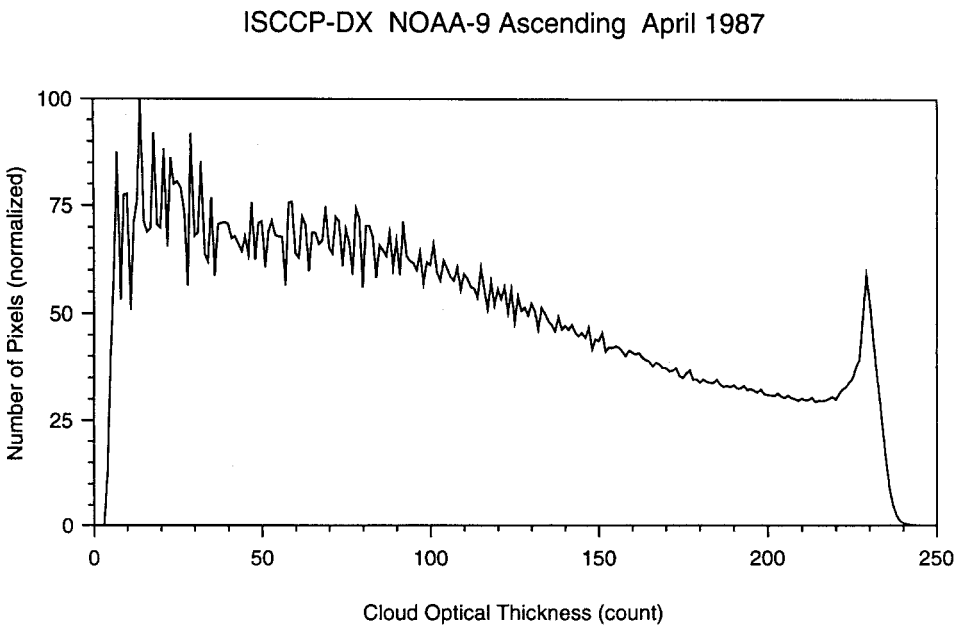

Fig. 3b.

Figs. 3(a)–(b). Frequency distribution over the whole globe of: (a) cloud optical thickness for April 1988; and (b) cloud spherical albedos (proportional to optical thickness count values in the ISCCP dataset) for April 1987 from ISCCP. In (a) individual values have been averaged over regions about 280 km in size, but in (b) the distribution of individual values is shown directly.

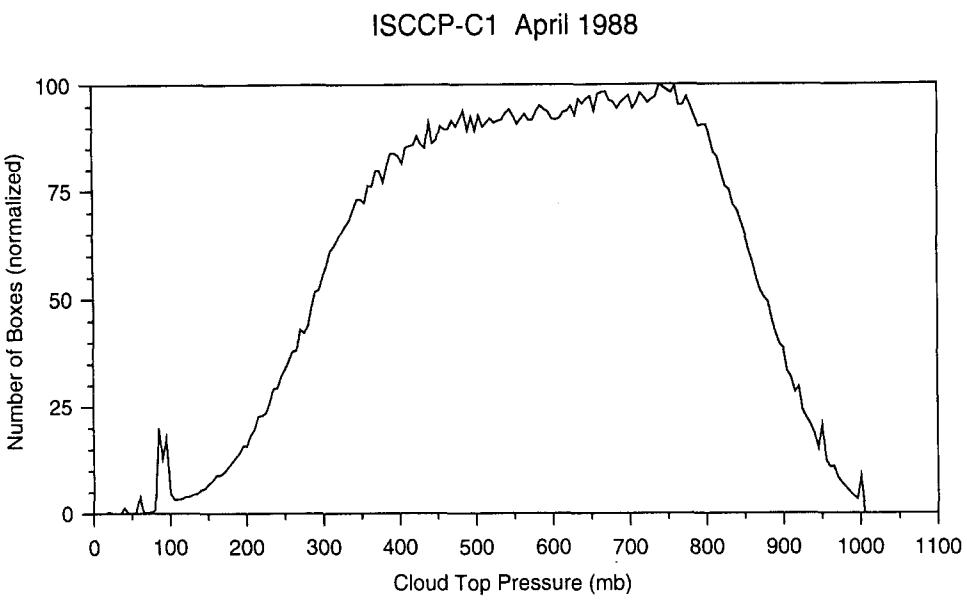

Fig. 4. Frequency distribution over the whole globe of cloud top pressure (in millibars) inferred by ISCCP every three hours in April 1988. Individual values have been averaged over regions about 280 km in size.

changes in the shapes of the distributions of cloud properties, e.g., changes in amounts of cloud types.

Since the effects of cloud changes on the radiation and hydrological budgets also vary with the environment in which the cloud occurs, monitoring must also describe changes in the geographic distribution of clouds. For example, a shift of cloud cover from land to ocean without changing the total would alter the radiation budget. Moreover, systematic diurnal and seasonal changes in solar radiation and atmospheric temperature also alter cloud effects on the radiation and hydrological budgets, so that monitoring must also describe the distribution of clouds relative to these two time scales. For example, a shift of cloud cover from day to night or from winter to summer without changing the total would alter the radiation budget. In fact, any significant correlation of cloud variations with systematic variations of the atmosphere and surface can be crucial to determining their effects on the climate because such variations would change the radiative and latent heating/cooling that drives the atmospheric circulation. That cloud variations are, themselves, controlled by the atmospheric motions guarantees that many such correlations are possible. These complex correlations give rise to the possibility of many feedbacks of clouds on the climate, making their determination crucial to accurate projections of climate change.

The advent of a new global, long-term satellite cloud climatology, produced by the International Satellite Cloud Climatology Project (ISCCP), makes possible the systematic investigation of the cloud variations, including changes in cloud cover,

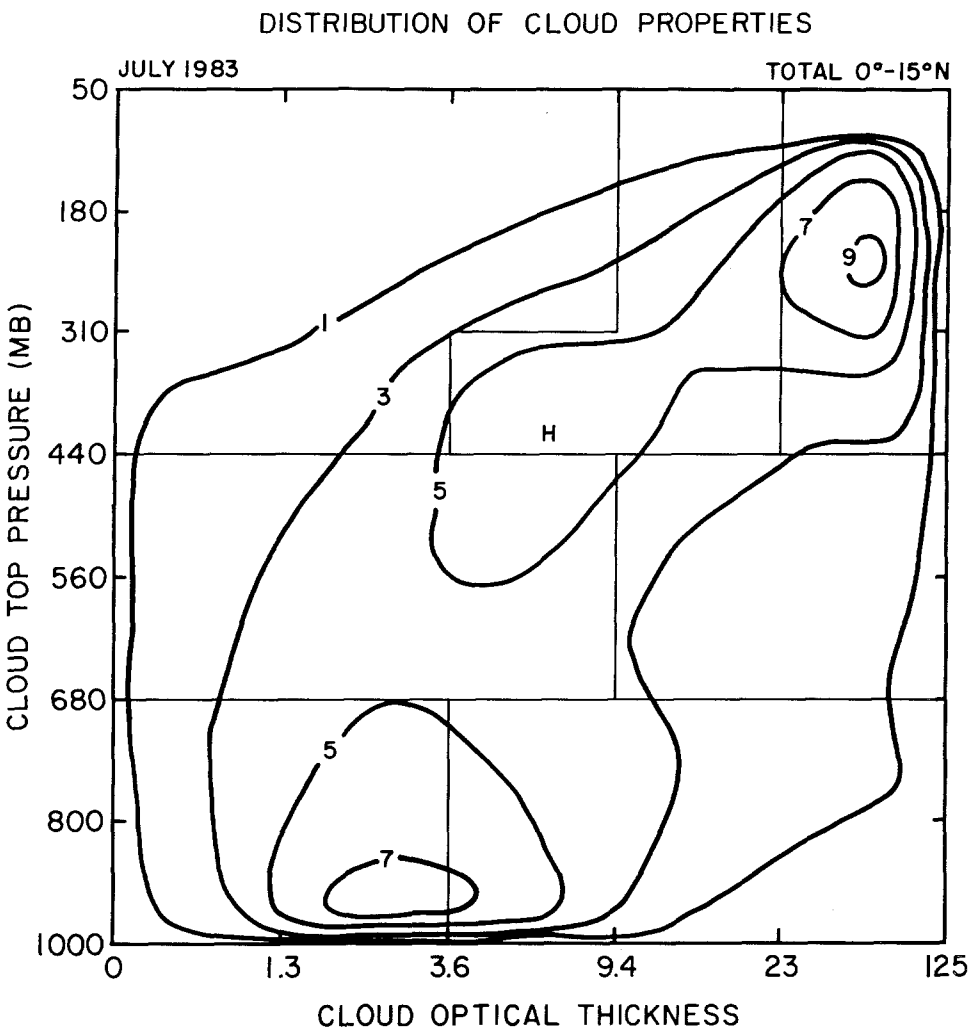

Fig. 5a.

top height (or pressure) and optical thickness (Rossow and Schiffer, 1991), over a very large range of space and time scales. These parameters are the main quantities governing the effects of clouds on Earth's radiation budget and are related to the main quantities that determine the role of clouds in the hydrological cycle. In particular, the cloud optical thickness, which is being measured systematically for the first time by ISCCP (cf. Rossow and Lacis, 1990), is a function of the cloud water content and vertical extent. This comprehensive dataset can also be used to draw together many previously isolated results to examine the full range of cloud variability. We review what is known about smaller scale cloud variations and illustrate some of the larger scale changes using the ISCCP dataset to determine the necessary characteristics of a cloud monitoring system.

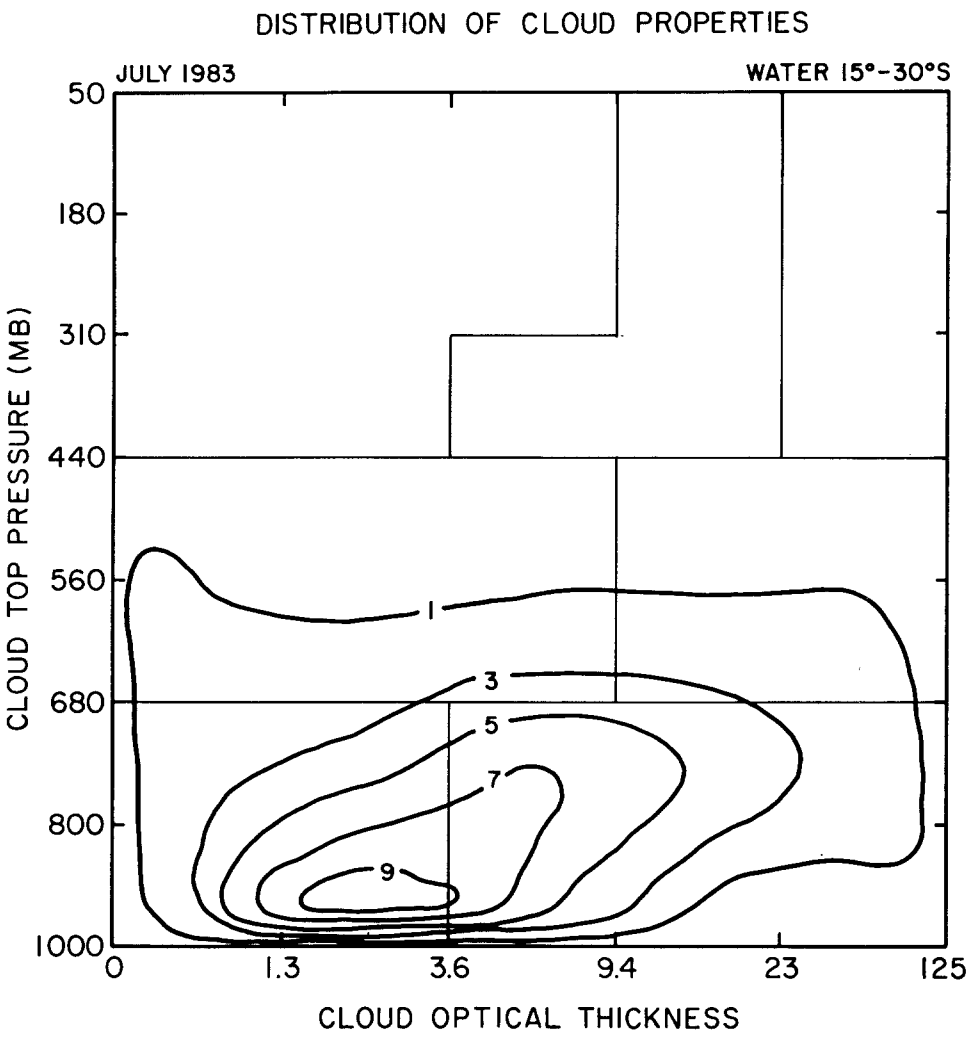

Fig. 5b.

2. Characteristics of Cloud Observing Systems

Clouds have been observed from the surface, from instrumented aircraft, and, most recently, from satellites. Each of these systems has characteristic space-time sampling patterns. Rawinsondes (Elliot and Gaffen, 1991; Gaffen *et al.*, 1991) and most lidars (cf. Sassen, 1991) provide vertical profiles at one point. The former are typically launched only once every 12 hr while the later make measurements with time resolution better than 10 s but only for short periods of time. Surface weather observers (Warren *et al.*, 1986, 1988) and typical radiometers and cameras describe the horizontal variations of clouds over a domain that is approximately 30–50 km across (Barrett and Grant, 1979). Most such data are available with time

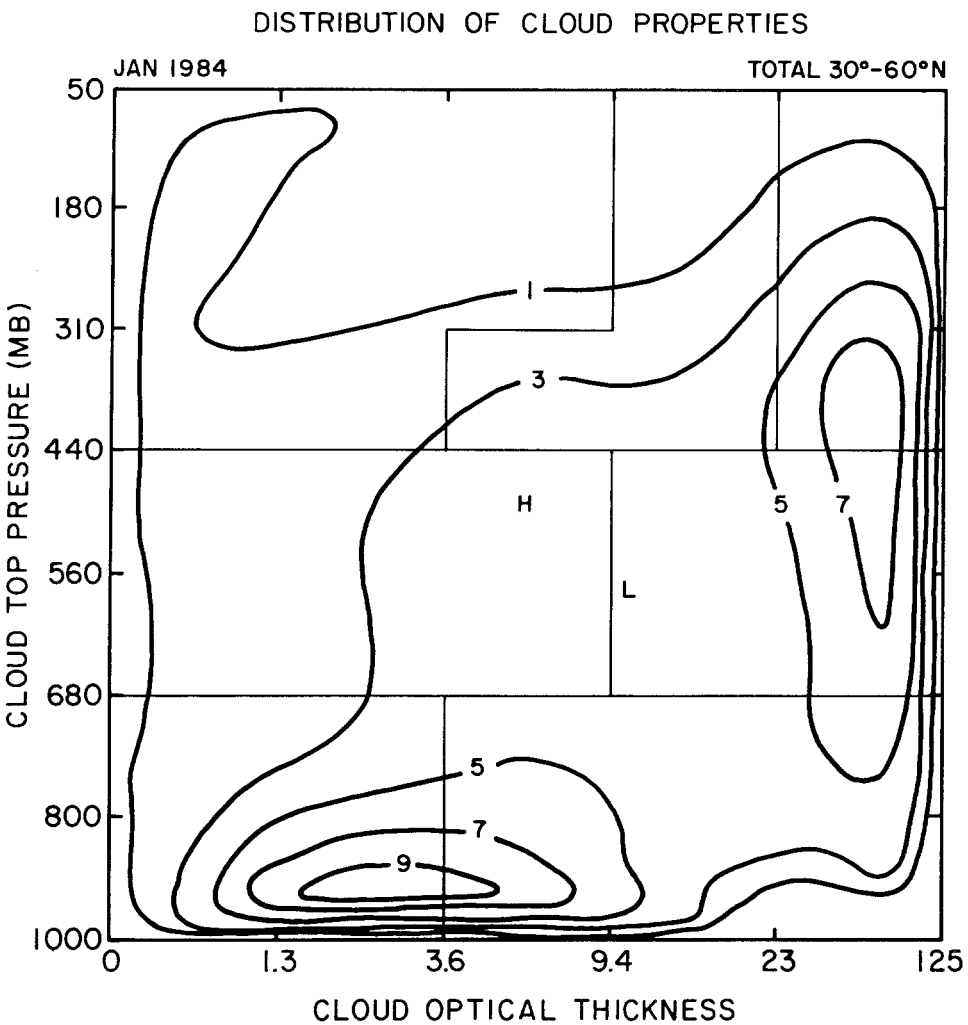

Fig. 5c.

Figs. 5(a)–(c). Two dimensional frequency distribution of cloud top pressure and optical thickness for three latitude zones: (a) the tropics between 0–15° N during July 1983; (b) subtropical oceans between 15–30° S during July 1983; and (c) northern midlatitudes between 30–60° N during January 1984. Contours indicate relative frequency with a peak value of 10.

resolutions of at least 3 hr. Radars (e.g., Houze *et al.*, 1989; Kropfli *et al.*, 1995) often scan a volume about 50–200 km across by 10–20 km deep with very high time resolution, though these data are not systematically analyzed. The major limitation of surface-based cloud datasets is that they are predominantly from populated land areas, leaving large portions of some continents and the oceans unobserved (Warren *et al.*, 1986, 1988). Collection of ship observations over many decades have probably provided accurate information for most of the northern hemisphere ocean,

however. Thus, surface cloud observations can be approximately characterized as providing long time records of point-like measurements with relatively high time-space resolution and relatively complete coverage of most land areas but incomplete global coverage. The only surface-based observations that have been analyzed systematically are surface weather observer reports (Warren *et al.*, 1986, 1988; Hahn *et al.*, 1994).

Aircraft can provide *in situ* cloud measurements with fairly high spatial resolution and can cover somewhat larger areas ($\sim$ 500 km) than observed from the surface; however, their spatial sampling is much poorer unless many aircraft work together and their time sampling is usually equivalent to a single sample. Aircraft can be used to probe either vertical or horizontal structures, but multiple aircraft are required to do both at the same time. Few systematic analyses of observations from a large number of aircraft cloud observations have been undertaken (cf., Cox *et al.*, 1987).

Satellite instruments more easily cover the largest space and time scales and provide a variety of cloud measurements (Rossow, 1989). Satellites in polar orbits can provide complete global coverage, albeit with relatively low time resolution ($\approx$ 12 hr for a single orbiter). On the other hand, satellites in geostationary orbit can provide very high time resolution ($\approx$ 15–30 min) over large areas; four to five such satellites can cover most of the globe up to latitudes of about 55° in each hemisphere. Spatial resolution is highest for the imaging radiometers: image pixel sizes for weather satellites range from 1–5 km. Although satellites intended to study land surfaces have resolutions of 10–30 m, such data are rarely collected and analyzed for the whole globe. The coupling of the space-time scales of cloud variations constrains the meaningful resolution of satellite observations (Salby, 1989). A polar orbiting instrument with a sampling of about 12 hrs can only meaningfully describe cloud variations on spatial scales > 1000 km. An instrument in geostationary orbit with a time resolution of 30 min can describe cloud variations down to spatial scales $\sim$ 5 km but cannot view scales $\gtrsim$ 5,000 km.

One interesting point regarding the issue of coupling of space-time scales is whether randomized sampling might provide a practical compromise between high resolution and aliasing. Theoretically, if truly random sampling in space and time were possible with a satellite observing system, unaliased estimates of the measured quantities could be obtained, but at the expense of substantially increased noise in the estimates of monthly mean quantities (Gaster and Roberts, 1977). This statement should be qualified by noting that most analyses of such issues presume that sampling is truly random, a Poisson point process, or a renewal process (Shapiro and Silverman, 1960), which would not be strictly true for a satellite observing system. Random sampling does not, therefore represent a universal panacea, particularly if noise is a concern.

Several comprehensive satellite cloud datasets now exist (Stowe *et al.*, 1988, 1989; Rossow and Lacis, 1990; Mokhov and Schlesinger, 1993, 1994), but the ISCCP datasets are higher resolution and report more cloud properties (Rossow

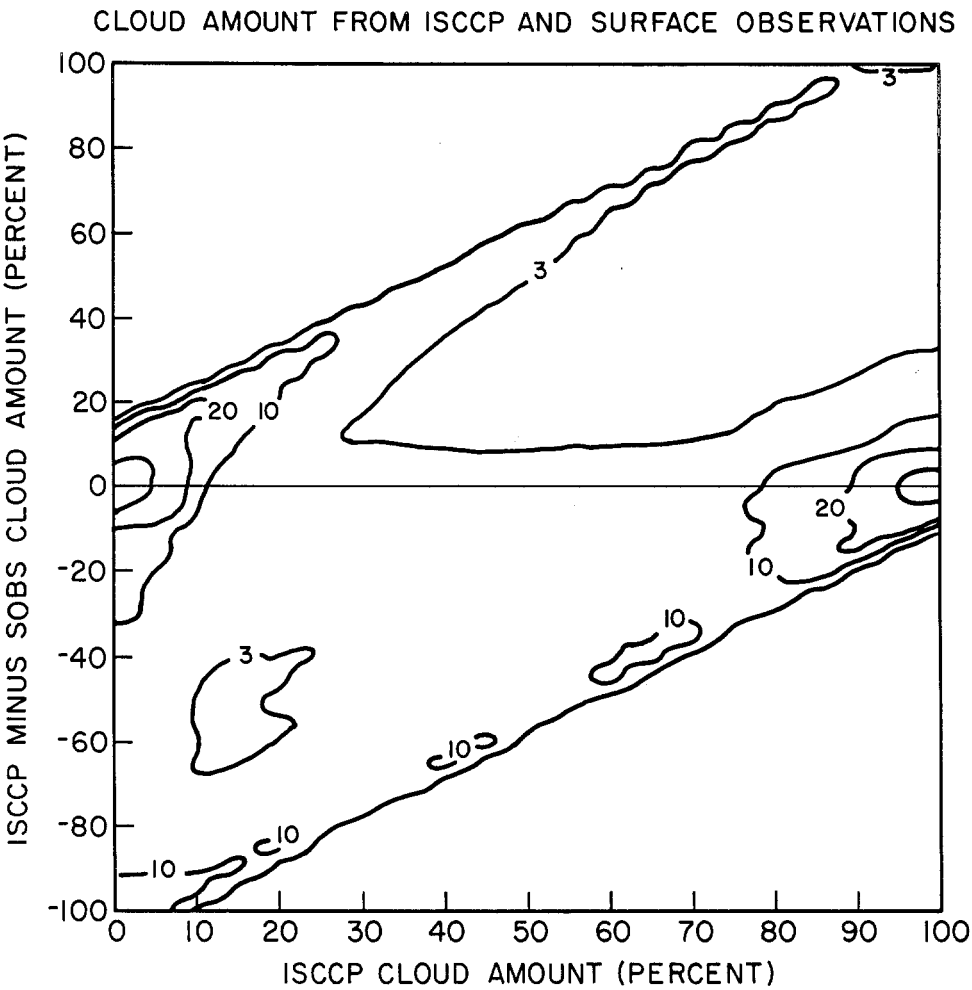

Fig. 6. Two dimensional frequency distribution of the difference between ISCCP and surface-observed estimates of cloud amount and the corresponding ISCCP cloud amount. Contours indicate frequencies in percent relative to the maximum value; unlabeled contours near (0,0) and (0,100) are for 50%.

and Schiffer, 1991). The ISCCP climatology is global, covers eight years at present, and has a space-time resolution of 30 km – 3 hr.

3. Characteristic Variations of Clouds

Comparison of cloud cover fractions determined at two different spatial scales, one about 50 km and one about 280 km, shows a trifurcation of the difference distribution (Figure 6)) when plotted against the cloud fraction from either source (Rossow *et al.*, 1993). The cases forming the two slanting branches are caused by stratiform

cloud types that either completely or partially cover the larger area observed from satellites and appear as either completely clear or completely overcast skies in the more 'point-like' surface observations. In other words, the cloud cover is partial only at larger scales. Since the location of the surface observer is essentially random within the larger domain, the disagreement between the two measurements is almost always the maximum possible when the larger area is only partially covered. The cases forming the horizontal branch with near-zero differences are caused by 'broken' cloud types that produce partial coverage at smaller scales. In this case, the disagreements between the two measurements appears random with little bias. The relative proportion of these groups is consistent with the populations of stratiform and cumuloform cloud types reported in surface observations over land (Warren *et al.*, 1986). This result implies significant numbers of clouds with sizes < 50 km and > 280 km. The practical limitations on surface and aircraft observations, as well as the cost of analysis of very high resolution satellite imgaes, has tended to divide cloud studies into those considering scales smaller than about 200 km and those considering larger scales.

3.1. SMALLER SCALE VARIATIONS

Many studies of the smaller scale structure of clouds have focused on the possible biases in estimating fractional cover using 'low' resolution satellite instruments. A recent study by Wielicki and Parker (1992) using LANDSAT images with a spatial resolution of 28 m shows that highly broken marine boundary layer clouds, characterized by size distributions with broad peaks in the range between 0.5 km and 5 km, are also characterized by a continuum of optical thicknesses (see also Cahalan *et al.*, 1994). There is also a tendency for the average optical thicknesses to increase as the average cloud cell size increases. In another study, lower average values of cloud cover (<0.3) are found to be associated with more frequent occurrence of lower optical thicknesses (Harshvardhan *et al.*, 1994). Consequently, the overestimate of cloud cover by counting cloudy pixels in lower resolution satellite images is partially offset by the failure to detect some of the optically thinner clouds (Wielicki and Parker, 1992). This means that the cloud detection threshold can be tuned *for a particular type of cloudiness* to obtain accurate cloud cover. The key implication of this result is that smaller scale cloud variations may be more appropriately considered in terms of variations of optical thickness, where clear sky is associated with the lowest value, rather than in terms of discrete objects with distinct and well-defined boundaries.

Cloud size distribution studies at spatial scales < 200 km have focused predominantly on marine boundary layer cloudiness (however, see Parker *et al.* (1986) for a study of land boundary layer clouds and Kuo *et al.* (1988) for a study of cirrus clouds). The size distributions are generally continuous power laws with negative exponents < –1 and often exhibit changes in slope in the size range from 0.5 km to 5 km that have been described as 'peaks' (Cahalan and Joseph, 1982; Parker

et al., 1986; Wielicki and Welch, 1986; Welch *et al.*, 1988: Joseph and Cahalan, 1990, Sengupta *et al.*, 1990; Weger *et al.*, 1992; Zhu *et al.*, 1992; Weger *et al.*, 1993; Lee *et al.*, 1994). These distributions are generally such that most of the area is occupied by the larger clouds (exponent > –2), except at scales smaller than the 'peak' scale, where the exponent approaches –3. Moreover, clustering also appears to be common. Organization of the smaller cloud elements into clusters $\sim$ 10–50 km in size suggests influence by the boundary layer dynamics. The study by Lee *et al.* (1994) also shows clustering at scales < 3 km, which they interpret as reflecting the dynamical forcing for convection. At intermediate scales (3–10 km), the spatial distribution appears random. In these particular results, the radiance threshold is selected at the median reflectivity, so that it is optical thickness variations that are being examined. The fact that the spatial distribution and size of the clusters resembles that of the larger cloud elements suggests instead that the clusters containing very small (< 1 km) elements are dissipating forms of the larger clouds. Since all of these studies are based on analyses of single images, the size spectra mix newly formed, mature and decaying clouds together in a way that may be misleading. There have been no studies that examine the correlation of the space and time variations of clouds at these smaller scales.

A key characteristic of these highly broken boundary layer clouds with very small elements may have been missed because all of the studies cited above use single views of domains that are only 100–200 km in size (the LANDSAT scene size). This characteristic was suggested by the sampling study of Seze and Rossow (1991a, b), where the radiance variation statistics of such clouds from 5 km resolution satellite images were compared with statistics from the same data sampled to spatial intervals of 30 km (like the ISCCP dataset). The quantitative similarity of these statistics was explained by assuming that such small-scale broken clouds tends to occur in 'fields' that are large enough (many hundreds of kilometers) that the sampled dataset still contains a sufficient sample to portray the variation statistics accurately. This conclusion requires that the small scale statistics be homogeneous over the larger spatial scale of the whole cloud field. That this might be true is suggested in the study of Lee *et al.* (1994), where the positions of the clouds and cloud clusters become essentially random at scales > 5 km. This conclusion needs further confirmation, but it explains the ability of the sampled ISCCP dataset to describe cloud amounts even for broken cloud types (Rossow *et al.*, 1993).

In general, the depth of the troposphere is only 10–15 km, so that typical cloud horizontal dimensions are far larger than their vertical dimensions, i.e., clouds form layers. Even the smaller boundary layer clouds tend to have vertical extents that are smaller than their horizontal dimensions. The dynamic coupling of atmospheric vertical structure to the horizontal distribution of clouds is often neglected in small scale studies, even though the boundary layer depth may well determine the horizontal size spectrum of the clouds over land and ocean (Kaimal *et al.*, 1976; Nicholls, 1989). An additional important feature of cloud vertical structure

is the frequent occurrence of multiple layer clouds. Surface observations suggest that at least half of cloud occurrences involve two layers (Warren *et al.*, 1985). A preliminary analysis of a limited rawinsonde dataset reaches a similar conclusion and notes that the typical separation distance of these two layers is of the same order as the average layer thicknesses (Wang and Rossow, 1995).

In the time domain the most important, coherent, high frequency variation of clouds is the diurnal cycle (Hendon and Woodbury, 1993; Salby *et al.*, 1991; Cairns, 1995). This is demonstrated in Figure 7 where we show the power spectra of cloud top pressures for the zonal average at a latitude of 45° N and for a single small region ($\approx$80,000 km^2) in southwest Europe at the same latitude. It is apparent from Figure 7b that mesoscale variability provides much more localized variability than the diurnal cycle. However mesoscale variability does not have the same global temporal coherence that the diurnal variations do. This is shown by Figure 7a where mesoscale variability is suppressed in this large scale average compared with the diurnal cycle. Thus, although the local variability explained by the diurnal cycle may not be as great as mesoscale variability, the spatially coherent phase of the diurnal cycle (Cairns, 1995) means that it is of particular importance when considering the sampling issues relevant to monitoring. The spectra shown in Figure 7 are estimated using a multitaper method with five windows and their variance is therefore well estimated by a chi-square distribution with ten degrees of freedom (Thomson, 1990). Since the spectra are logarithmically plotted the reader can readily estimate confidence intervals that apply to any frequent point (Priestly, 1981). The only significant line components in these spectra are the diurnal and semi-diurnal components.

A better understanding of the smaller scale temporal variability of clouds and their regional variations can be obtained from an EOF analysis of global, daily mean maps of cloud amount, optical thickness and cloud top pressure. Using a 90-day record from boreal spring, we find that local day-to-day variations account for about 60% of the variability, more than the time-mean regional variations; however, these rapid time variations mostly form a 'noise-like' distribution of principal components, each of which only explains 1–2% of the variance. This indicates little global coordination of the higher frequency (daily) cloud variations.

As already suggested in Figure 7, the diurnal cycle is the strongest coherent variation of clouds on time scales less than one season. The relative importance of the diurnal variations compared with lower frequency fluctuations can be evaluated by fitting a model, consisting of a mean, a diurnal and a semi-diurnal component, to the seasonally averaged diurnal variation of clouds from the ISCCP dataset. Although there is some variation in the relative strength of the three terms for different seasons and cloud types, approximately 75% of the global cloud variation is explained by the seasonal mean, 15% is explained by the diurnal component, and 5% is explained by the semi-diurnal component (Cairns, 1995). The magnitude and phase of the diurnal cycle are highly variable with location and the diurnal cycle is not a simple harmonic oscillation (Kondragunta and Gruber, 1994; Cairns, 1995).

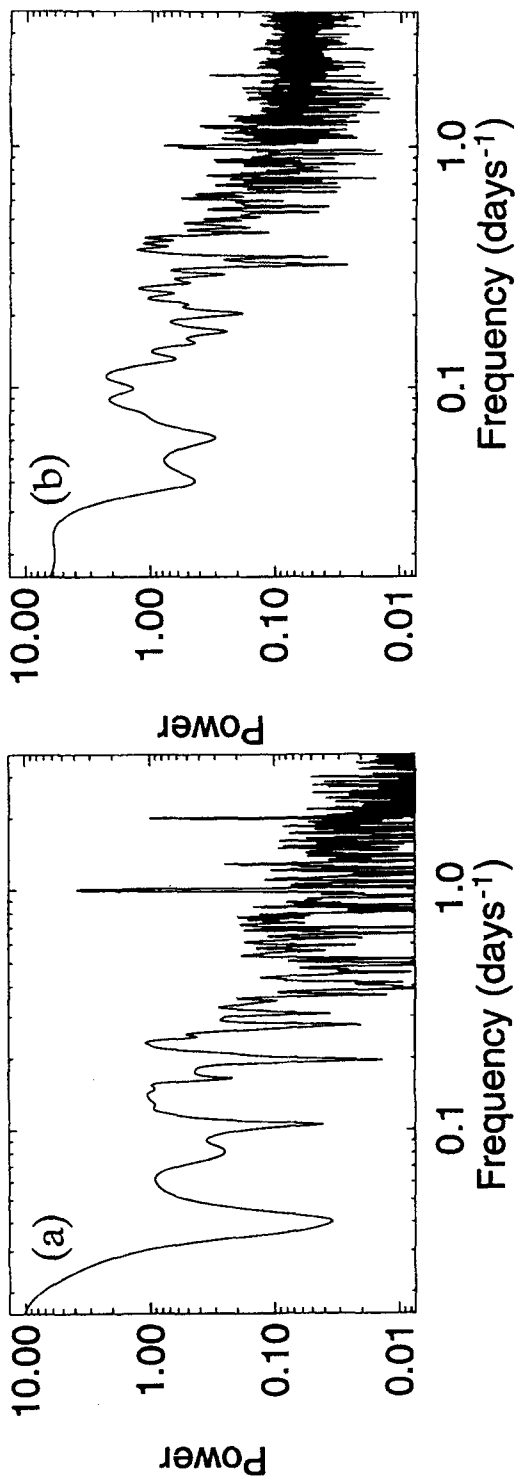

Fig. 7 Temporal spectra of cloud top pressure variations for December 1987 to March 1988 from measurements at three hour intervals (ISCCP C1 data). (a) Spectrum of a time series that was interpolated and then shifted to local time at each longitude and spatially averaged around the entire 45° N latitude zone; (b) Spectrum of a time series that was averaged over a 400 × 400 km^2 area in southwest Europe at the same latitude as (a).

Low cloud amount over land has a well-defined diurnal maximum near 1330 Local Standard Time (LST), while over oceans there is broad maximum near 0800 LST. The amplitude of low cloud variation is approximately 10–15% over land areas, but only a few percent over oceans (Carlson *et al.*, 1995). Middle-level cloud amount has a maximum at around 0500 LST over tropical land areas while high cloud amount peaks between 1800 LST and midnight. Over oceans in the convergence zones (Intertropical – ITCZ, South Pacific – SPCZ, South Atlantic – SACZ), high cloud amount is maximum in early evening (1600 to 2000 LST), but there is also an early morning maximum in deep convective clouds (Fu *et al.*, 1990). The amplitude of diurnal variations of middle- and high-level clouds are generally <5% on average (Carlson *et al.*, 1995). The principal seasonal variation in the geographic distribution of larger diurnal amplitudes is for the summer hemisphere to have the stronger diurnal cycles. The asymmetry of the diurnal cycle, its varying phase with cloud type, and its amplitude and phase variations with location all emphasize the importance of proper sampling of this time scale in any cloud observations to prevent aliasing of these scales into low frequency variability.

3.2. LARGER SCALE VARIATIONS

Figure 2 shows that the cloud amount frequency distribution is bimodal, even at a spatial scale of 280 km (equivalent to 2.5° latitude-longitude at the equator), and that 15% of cloud systems are large enough to completely cover an area of this size (Figure 2 shows observations over land; over ocean more than 30% of clouds are large enough to completely cover 280 km areas – Rossow and Schiffer, 1991). Figure 8 shows the evolution of the ISCCP cloud amount frequency distribution in three latitude zones as the observations are averaged over progressively larger areas. In the tropics (Figure 8a), a nearly monomodal distribution with a peak near 50% is apparent when the observations are averaged over 10° latitude-longitude; however, there are still occurrences of complete overcast even at this scale ($\approx$ 1100 km). In northern midlatitudes a mode at about 75% only appears in the distribution averaged over 20° , but completely overcast cases are still frequent (Figure 8b). In southern midlatitudes where average cloud amount is very high, there is only a suggestion of a mode at 90% in the distribution averaged over 20° (Figure 8c). The monomodal distribution shape appears at a smaller scale in the tropics than in midlatitudes, but all distributions begin to exhibit this shape at a scale of $\approx$ 2200 km.

A complementary way to examine the large scale variability of clouds is to look at the spatial spectrum around a latitude circle (Zangvil, 1975): Figure 9 shows representative spectra at the equator, 30° N and 45° N. Each spectrum is formed from 100 realizations, which are the 3 hr ISCCP maps of cloud amount for the winter season of 1987–1988, and estimated using a multi-taper method (Thomson, 1990). The gross behavior of the spectrum is a power law with an exponent near –2; the –5/3 line representing a Kolmogorov turbulence spectrum

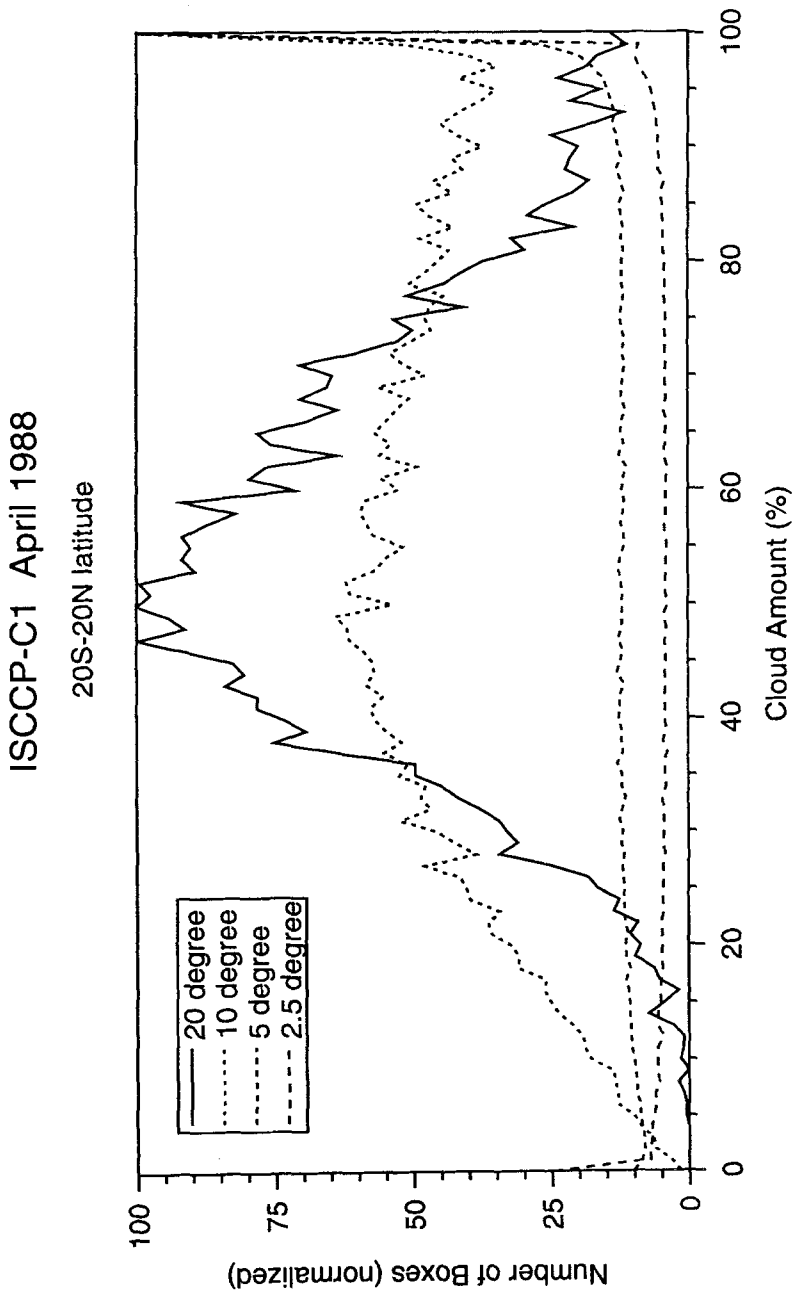
ISCCP-C1 April 1988
20S-20N latitude
20 degree
10 degree
5 degree
2.5 degree
Number of Boxes (normalized)
0
25
50
75
100
0
20
40
60
80
100
Cloud Amount (%)

Fig. 8a.

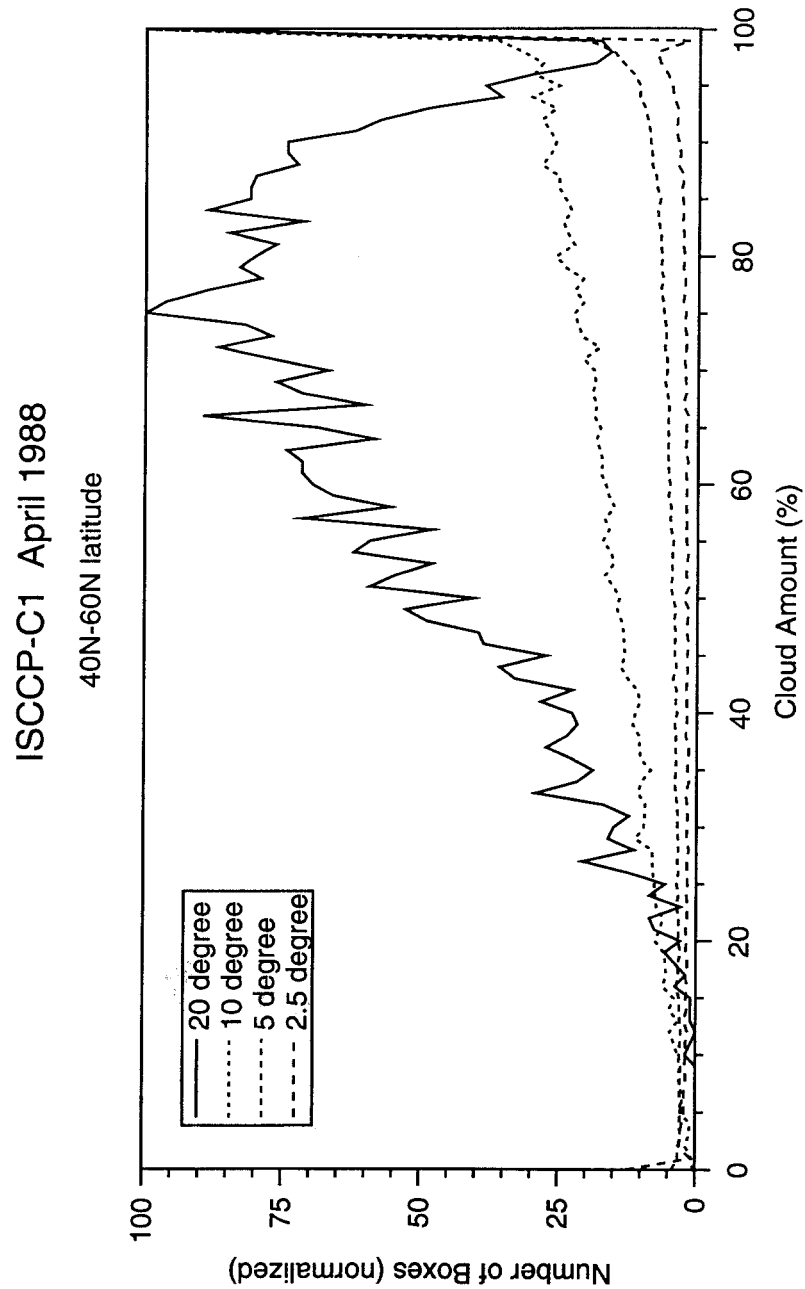
ISCCP-C1 April 1988
40N-60N latitude
20 degree
10 degree
5 degree
2.5 degree
Number of Boxes (normalized)
0
25
50
75
100
0
20
40
60
80
100
Cloud Amount (%)

Fig. 8b.

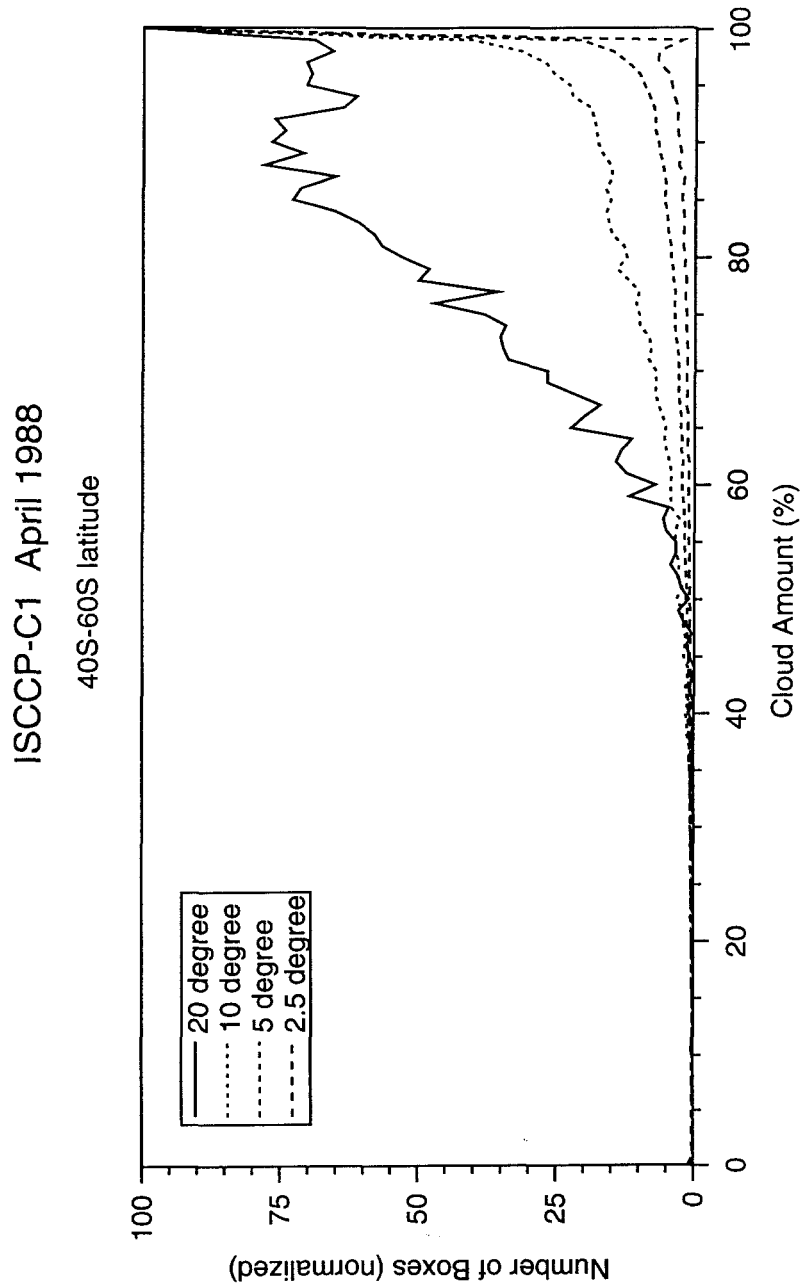

Fig. 8(a)–(c). Frequency distributions of ISCCP cloud amounts at three hour intervals for April 1988 averaged over four different map resolutions: 2.5°, 5.0°, 10° and 20° in the latitude zone (a) 20° –20° N; (b) 40° N–60° N; and (c) 40° S–60° S.

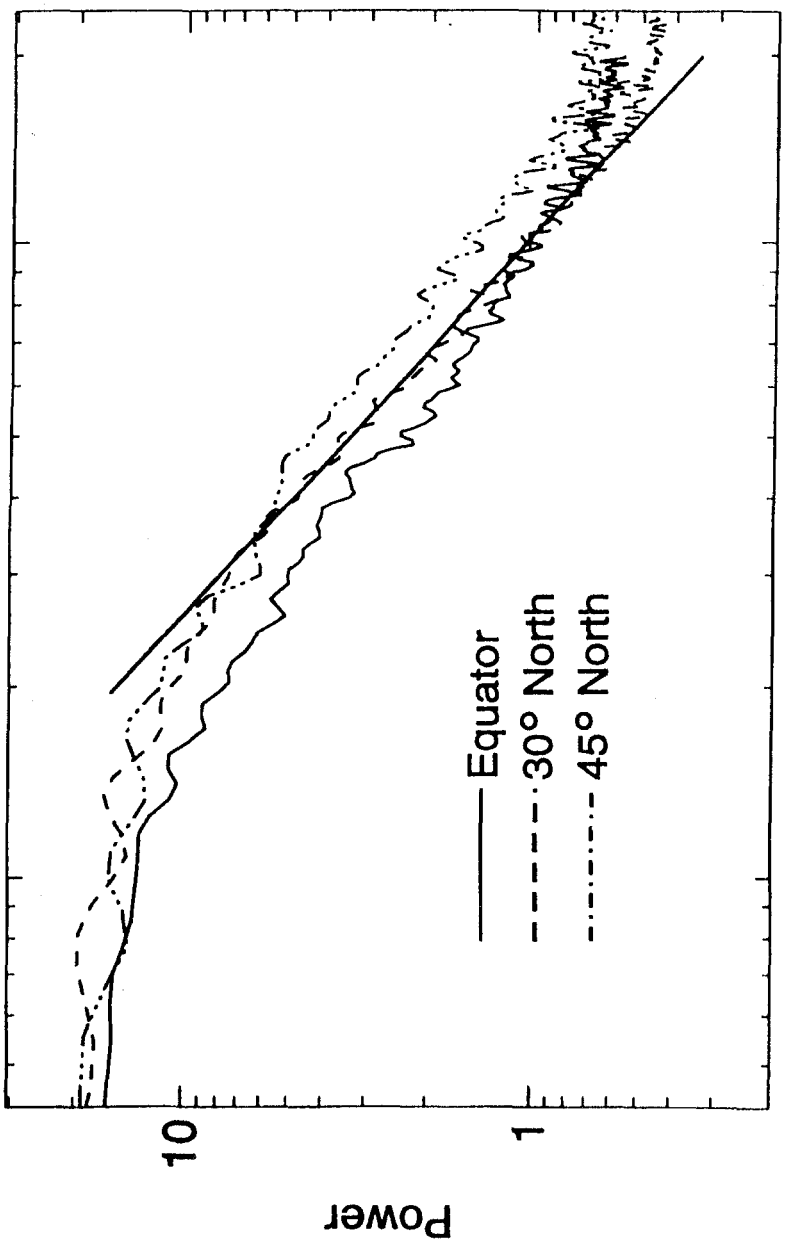

Fig. 9 Spatial power spectra of ISCCP cloud amount variations averaged over 100 'snapshots' at three hour intervals for the equatorial zone (solid line), 30° N (dashed line) and 45° N (dash-dot line). A straight solid line with a slope of –5/3 is shown for reference.

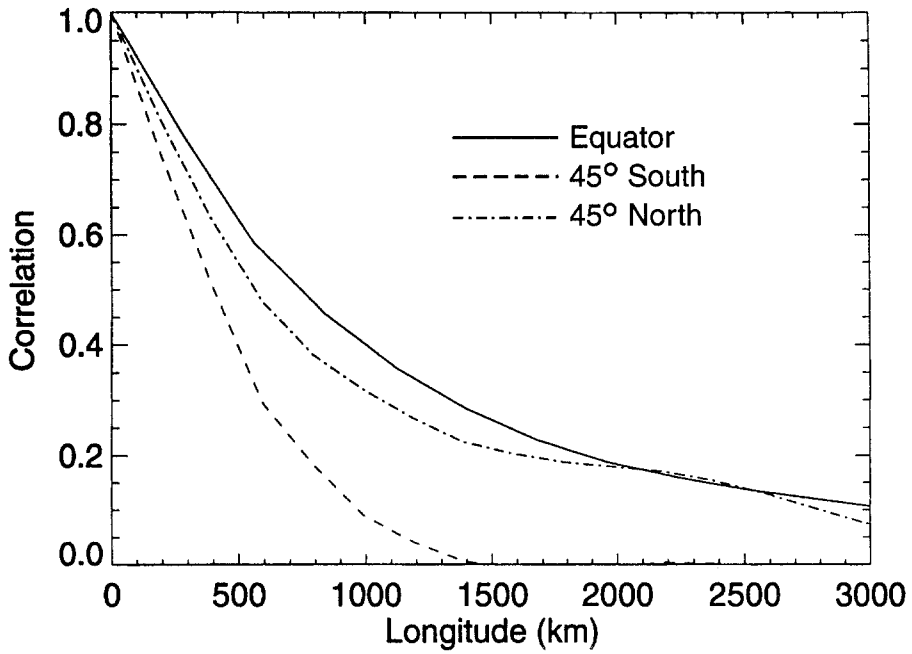

Fig. 10. Circular autocorrelation functions of ISCCP cloud amount variations averaged in a Z-statistic, where $Z = 0.5\log_e[(1+r)/(1-r)]$, over 100 'snapshots' at three hour intervals for the equatorial zone (solid line), at 45° S (dashed line) and at 45° N (dash-dot line).

is shown for reference. The power law appears to break down at an outer scale of $\approx$ 5000 km. Another way to examine the higher frequency behavior of cloud amount is through the circular function, which is shown for the equator and 45° N and S in Figure 10. These correlation functions are also the averages of 100 realizations at 3 hr time resolution. At the equator the correlation length scale is $\approx$ 1000 km, but at midlatitudes it is only $\approx$ 750 km and $\approx$ 500 km in the north and south, respectively. Despite the somewhat smaller size of cloud systems in the tropics suggested by Figure 8, these tropical systems appear to be coordinated by the longer waves so as to produce a somewhat larger correlation length scale. The shorter correlation length scales for **variations** in southern midlatitudes as compared with northern midlatitudes reflects the weaker stationary wave activity in that hemisphere: the stationary waves are generally longer wavelength than the transient waves (Pandolfo, 1993). Even with a smaller correlation length scale, the cloudiness is generally more nearly complete in southern midlatitudes (cf. Figure 8c).

The tendency of clouds to form 'thin' layers (i.e., to have vertical extents smaller than their horizontal extents) is illustrated by comparing the variability of ISCCP cloud top pressures within small local regions of about 280 km size with the geographic variation of cloud top pressures averaged over these small domains (Figure 11). Generally, the local variations of cloud top pressure are less than half

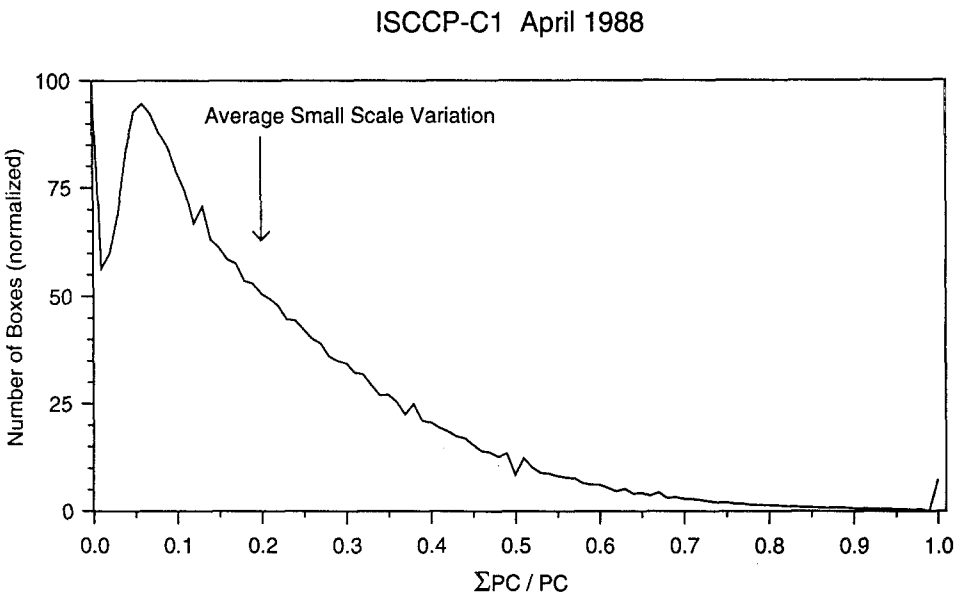

Fig. 11. Frequency distribution of the subgrid scale (< 280 km) standard deviation (ΣPC) of ISCCP cloud top pressures normalized by the corresponding mean cloud top pressure (PC). The standard deviation of the mean values over the globe is indicated by an arrow.

as large as they are from region to region; however, there is a significant number of systems with much larger local varibilities. In contrast, the magnitude of local variability of cloud optical thickness (not shown) is only about one quarter of the regional variations.

The importance of cloud top pressure variations is also apparent in its temporal power spectrum, averaged around the equator, when compared with the power spectrum of cloud amounts (Figure 12). The suppressed diurnal and semi-diurnal cycles in ISCCP total cloud amount result from the different phases of different cloud types (Cairns, 1995); however, these changes of cloud types appear as stronger, more coherent changes in the cloud top pressure over the day in the tropics (cf. Fu *et al.*, 1990). The suppression of the diurnal cycle in cloud amount is also related to the averaging with longitude: Figure 13 shows the autocorrelation of the zonally averaged cloud amount time series (solid line) and of a small region in equatorial Africa. The zonal average ISCCP cloud amount is correlated over $\approx$ 2 days while the correlation over Africa exhibits a diurnal fluctuation. Unlike the midlatitude example (Figure 7), the diurnal cycle is more apparent locally in the tropics because phase differences among different locations nearly eliminate any variation in the zonal average. This demonstrates, again, the association of short time scales with small spatial scales.

The larger scale (> 30 days) temporal variability of clouds can be compared to their regional variations by employing an EOF analysis of global, monthly mean

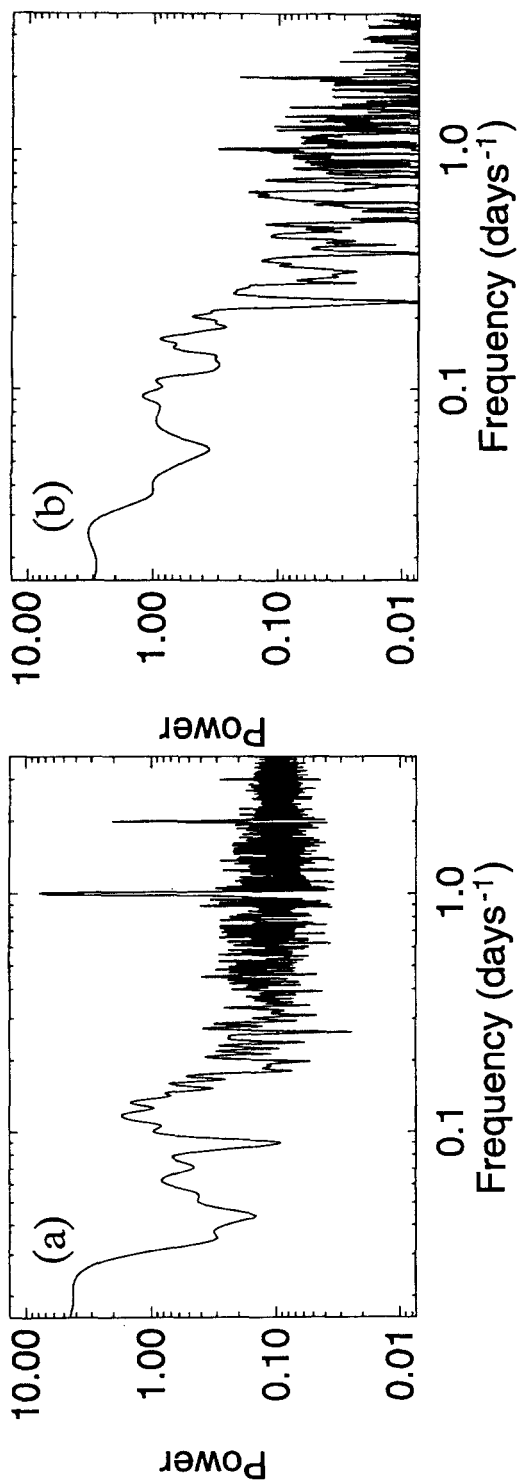

Fig. 12 Temporal power spectra of ISCCP cloud top pressures (a); and cloud amounts (b) for the period December 1987 to March 1988, using three hour samples. The data were interpolated and then shifted to local time at each longitude and spatially averaged around an equatorial zone 5° wide.

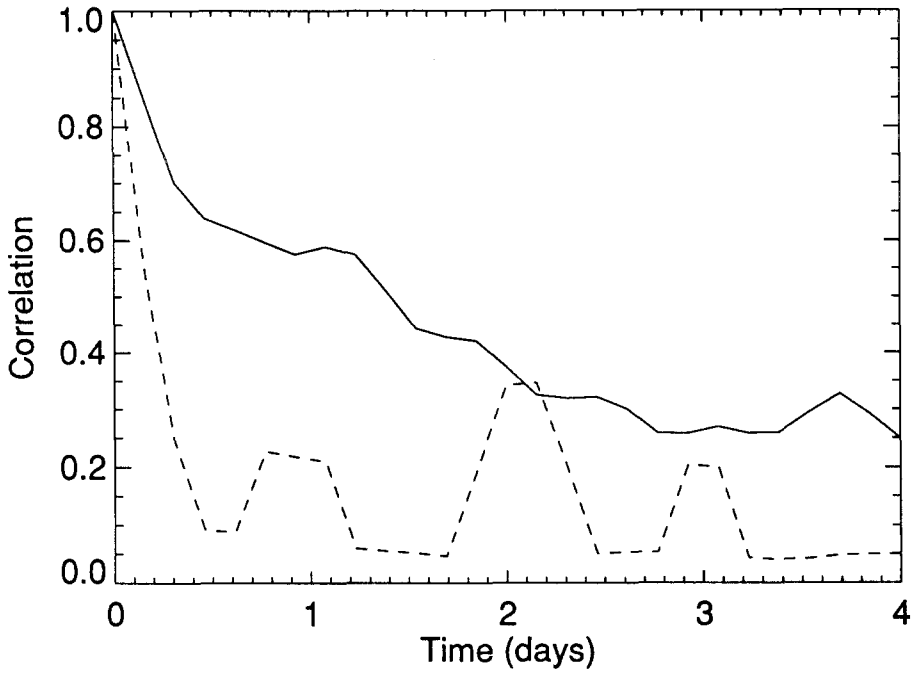

Fig. 13. Temporal autocorrelation functions of cloud amount variations for December 1987 to March 1988, using three hour samples from ISCCP for a time series that was interpolated and then shifted to local time at each longitude and spatially averaged around the equatorial zone (solid line) and a time series that was averaged over a 500 × 500 km^2 area in equatorial Africa at the same latitude (dashed line).

maps of cloud amount, optical thickness and cloud top pressure from ISCCP. We find that the first principal component of all three cloud properties is the time mean geographic variation (Figure 14). In the case of cloud amount and cloud top pressure, the regional variations account for about 65–70% of the total variance; but regional variations of cloud optical thickness account for only about 35% of the total. The next two principal components represent the annual cycle of cloud properties (Figure 14), accounting for another 15% of the variance of cloud amount and top pressure. The annual cycle of cloud optical thickness, on the other hand, accounts for almost 25% of the total variance. A few percent of the variation of cloud top pressure and optical thickness appears in a semi-annual cycle. Over longer periods of time, the dominant fluctuation in cloud properties is associated with the El Niño/Southern Oscillation (ENSO) phenomenon that accounts for 2–4% of the total variation in high cloud amount. The temporal variation of the 'ENSO' eigenvector of high cloud amount is shown for the NIMBUS-7 and ISCCP data records in Figure 15. That these variations are associated with the ENSO variation can be deduced only from the combined data record – each dataset alone has only one example making the interpretation ambiguous – showing the value of long continuous data records for diagnosing climate change.

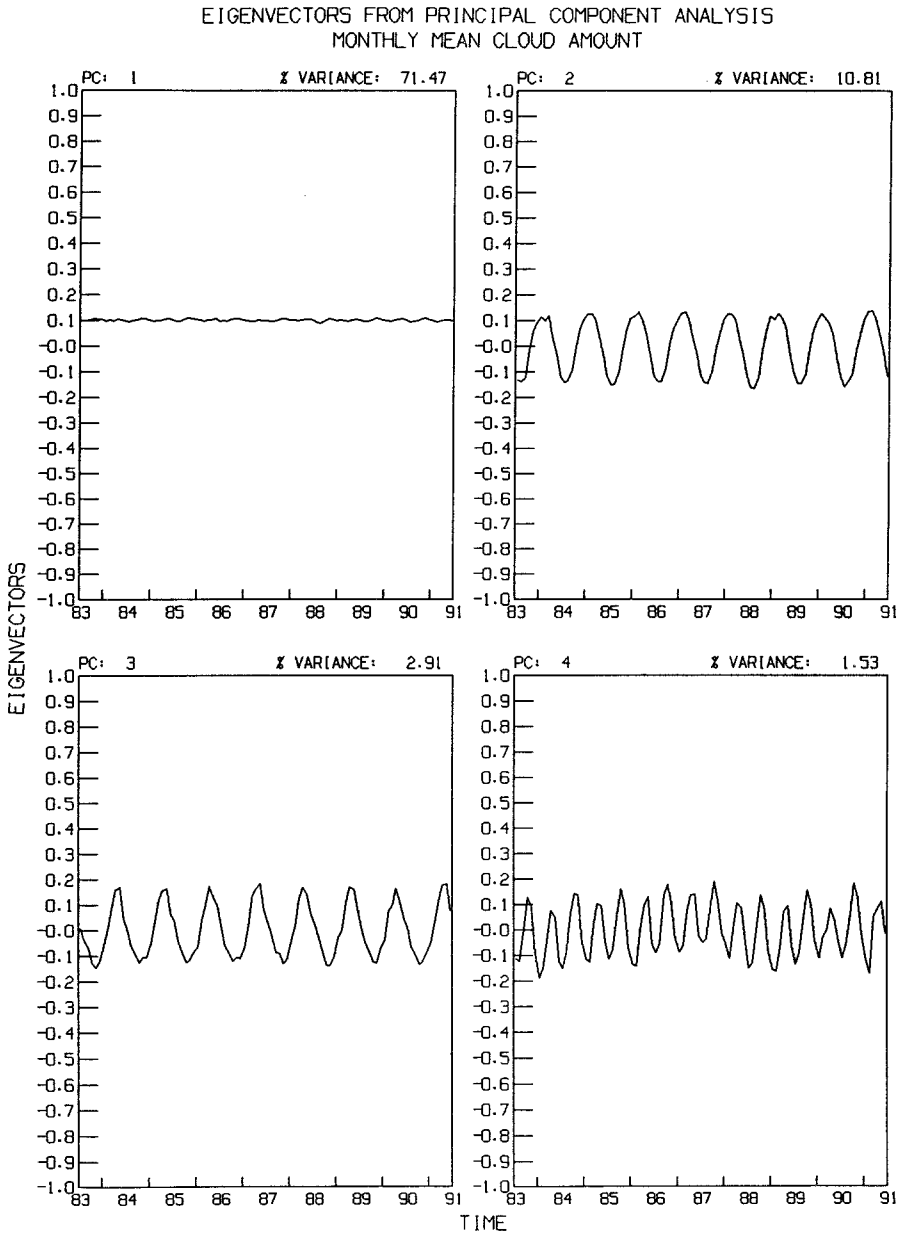

Fig. 14a.

Figure 16a shows an infrared image of the western equatorial Pacific region from GMS-4 satellite with a spatial resolution of 5 km (these data were prepared for the TOGA-COARE, Flament and Bernstein, 1993). This area was selected to illustrate the coupling of space and time scales because it is dominated by smaller

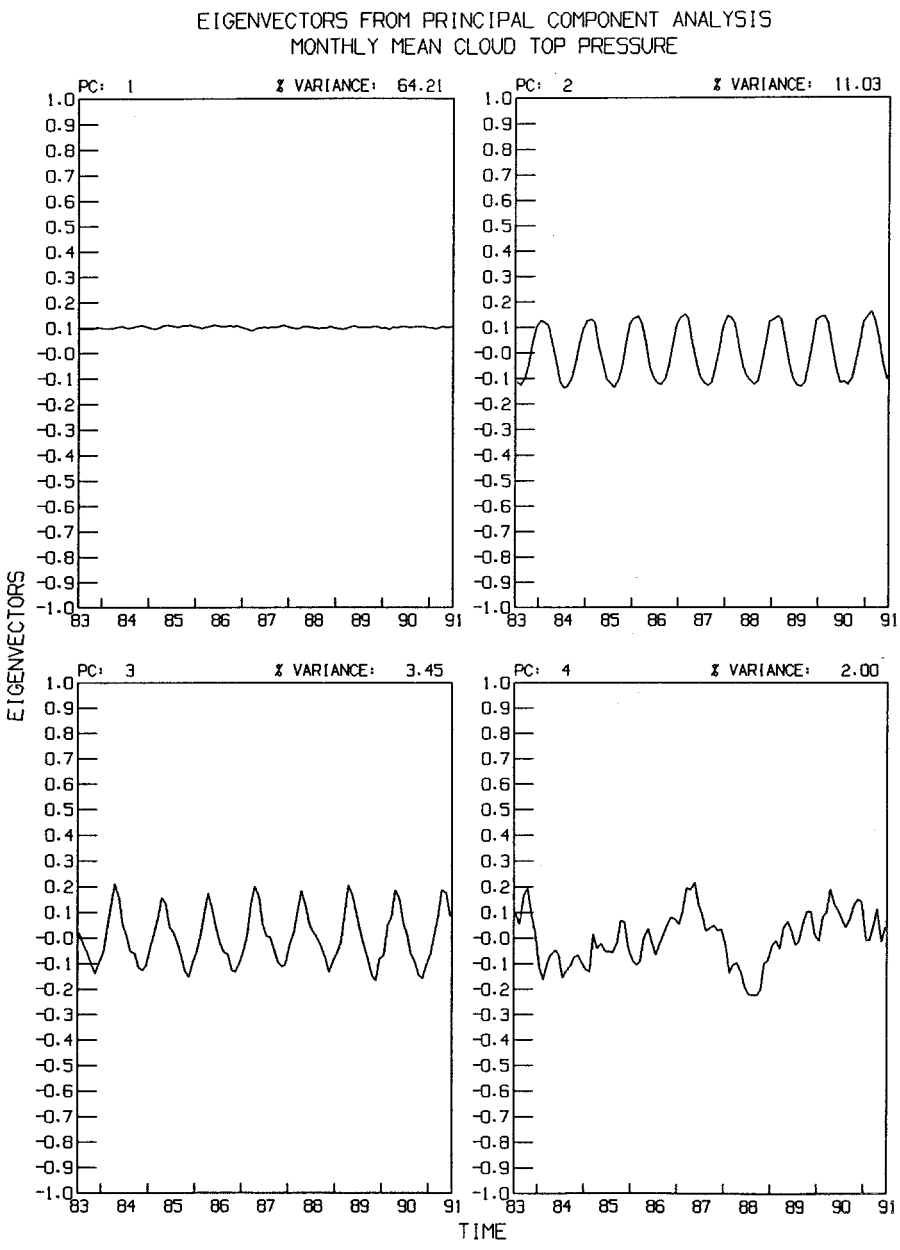

Fig. 14b.

scale motions and convective cloud structures. Hourly images like the one in Figure 16a are averaged over different time intervals: Figures 16b and 16c show the 24-hr and 240-hr averages. The visual impression of 'smoothing' or removal of smaller spatial scales as the averaging time period is increased is quantified in Figure 17,

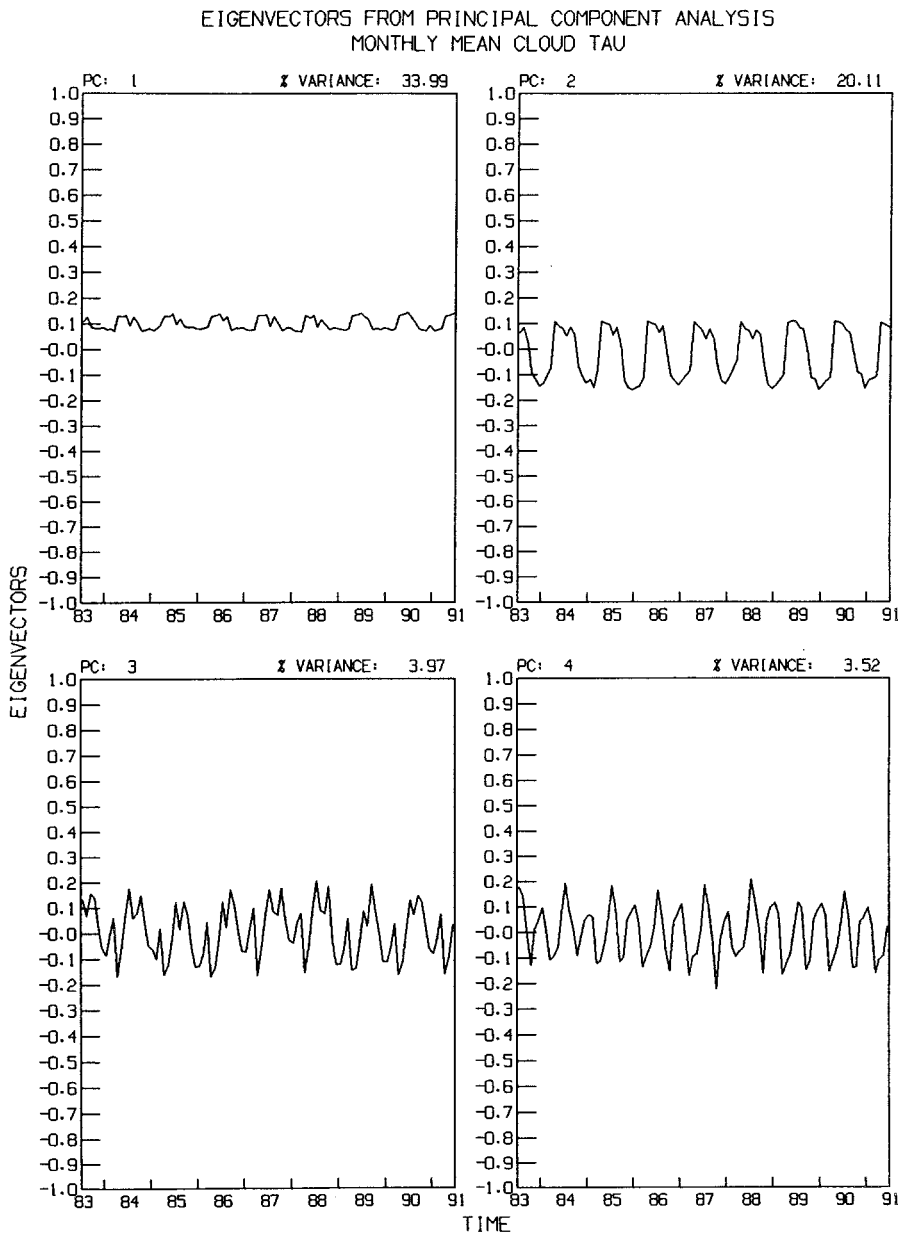

Fig. 14c.

Figs. 14(a)–(c). Time series derived from a principal components analysis of ISCCP global, monthly mean data for the period July 1983 to June 1991 for: (a) cloud amount; (b) cloud top pressure; and (c) cloud optical thickness. The first four significant eigenvectors are shown and the percent of the total variance that they explain is indicated.

which shows the evolution of the one dimensional Fourier power spectra. Most of the power is actually at spatial scales > 500 km, despite the visual predominance of small scale 'texture'. This means that the dominant variations of clouds that cause significant changes in radiative fluxes occur at these larger space scales. The slope of the spectrum is about –5/3 at scales larger than 300 km, but about –2.5 at smaller scales. Time averaging reduces the power at all scales < 500 km by at least one order of magnitude. Notably, there is not much difference between the spectrum for 24-hr and 72-hr averaging periods, suggesting little spatial variability associated with times in this range. Most of the spatial variability at scales < 500 km is eliminated when averaging over one complete diurnal cycle, but about half the decrease is produced by averaging over 3 hr for scales < 100 km. The largest scales (> 1000 km) are not affected until averaging over 240 hr. The spectral slope of the time-averaged data is about –2.

4. Sampling Uncertainties

Monitoring of long-term changes in global cloudiness that are **significant** to climate change requires observations that provide adequate sampling of the variability of clouds described above. The requisite statistical accuracy obtained from a cloud observing system can be estimated by determining the magnitude of changes in global mean cloud properties that would produce changes in the mean radiation balance of Earth that are >0.5 Wm^{-2}, about 25% of the forcing already produced by increased greenhouse gas abundances (cf. Hansen *et al.*, 1993). Based on calculations of the radiation budget using the observed atmospheric, surface and cloud properties (see also Zhang *et al.*, 1995), such a change in the radiation budget would be produced by changes of cloud amount, top pressure, optical thickness and particle radius of $\approx 1\%$, ≈ 10 mb, ≈ 0.15 and ≈ 0.3 μm, respectively. Figure 18 shows a possible 'signal' that should be detected by a cloud monitoring system: the eight year record of global cloud cover (deviation from the mean) from ISCCP shows a slow variation of $\pm$ 2% that appears to be associated with the 'cycle' of El Niño events during this period (see Figure 15). The $\sim$ 1% variations on shorter time scales (roughly month-to-month) may represent the 'noise-level' in these results.

If the purpose of monitoring cloud changes goes beyond merely detecting change to diagnosing the effects of the change, then the observing system must not only provide sufficient sampling density but also provide **complete** global coverage. The reason for this additional requirement is that, even when the global mean cloud cover does not change, the location of the clouds can: incomplete observation of the globe would not distinguish between these two cases. To illustrate the effect of partial coverage, we re-calculated the 'global' monthly mean cloud amounts from the ISCCP dataset shown in Figure 18 using the spatial coverage obtained in the analysis of surface temperatures by Hansen and Lebedeff (1988),

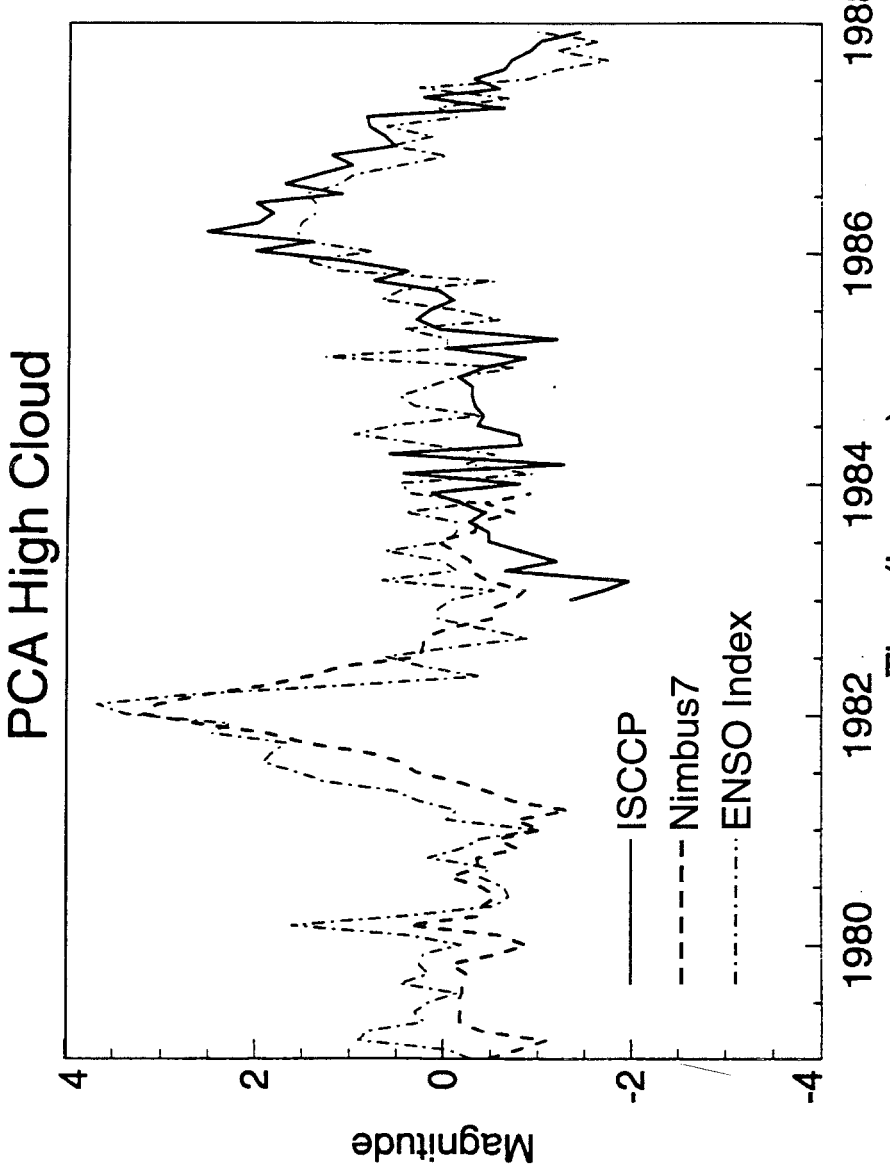

Fig. 15. Time series associated with the first principal components from the ISCCP (solid line) and Nimbus 7 (dashed line) of monthly mean high cloud amount anomalies. The dash-dot line shows the Southern Oscillation index (difference between sea level pressure at Darwin and Tahiti). The principal component analysis was applied to the global gridpoint normalized data sets.

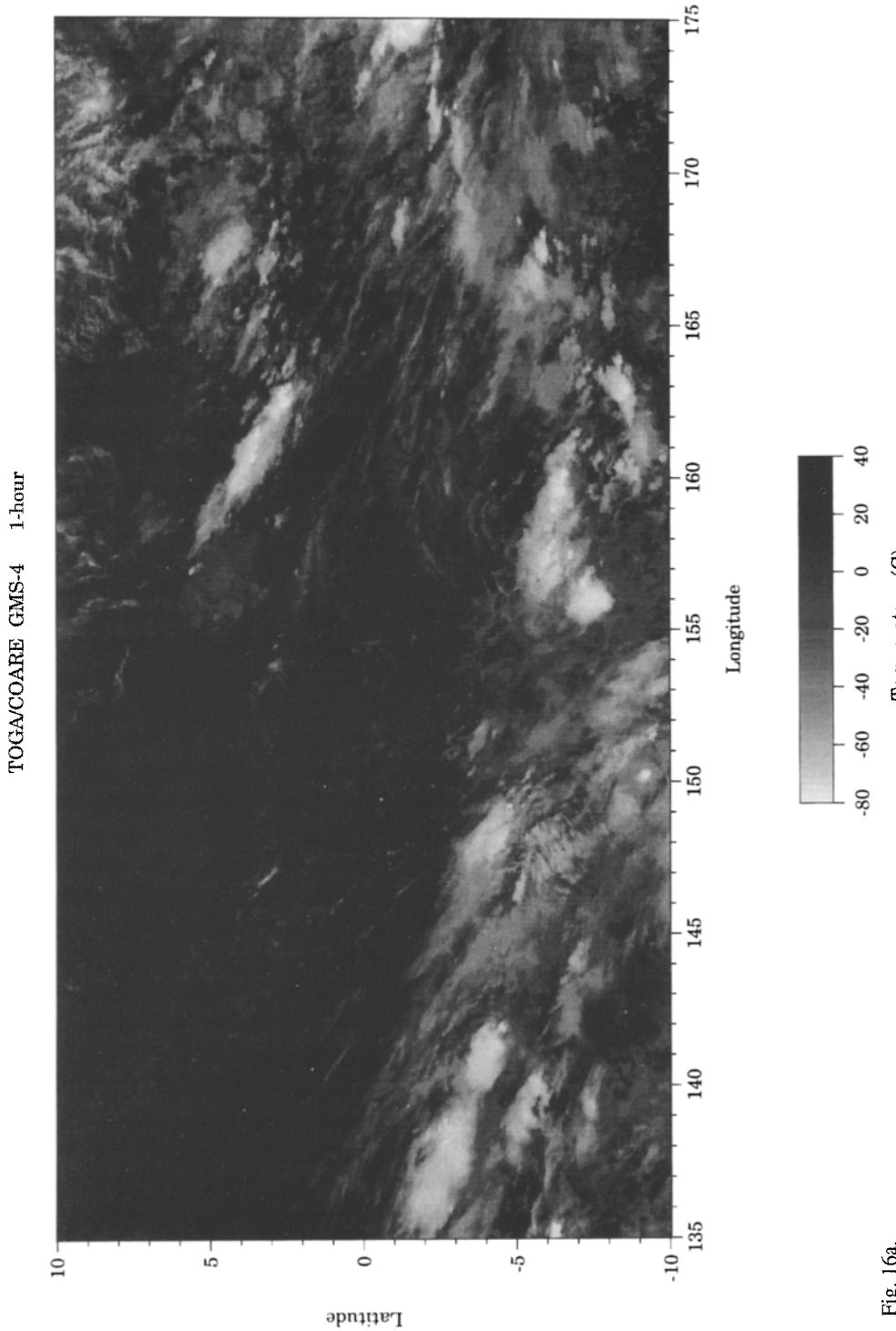
TOGA/COARE GMS-4 1-hour
Latitude
10
5
0
-5
-10
135
140
145
150
155
160
165
170
175
Longitude
-80
-60
-40
-20
0
20
40
Temperature (C)

Fig. 16a.

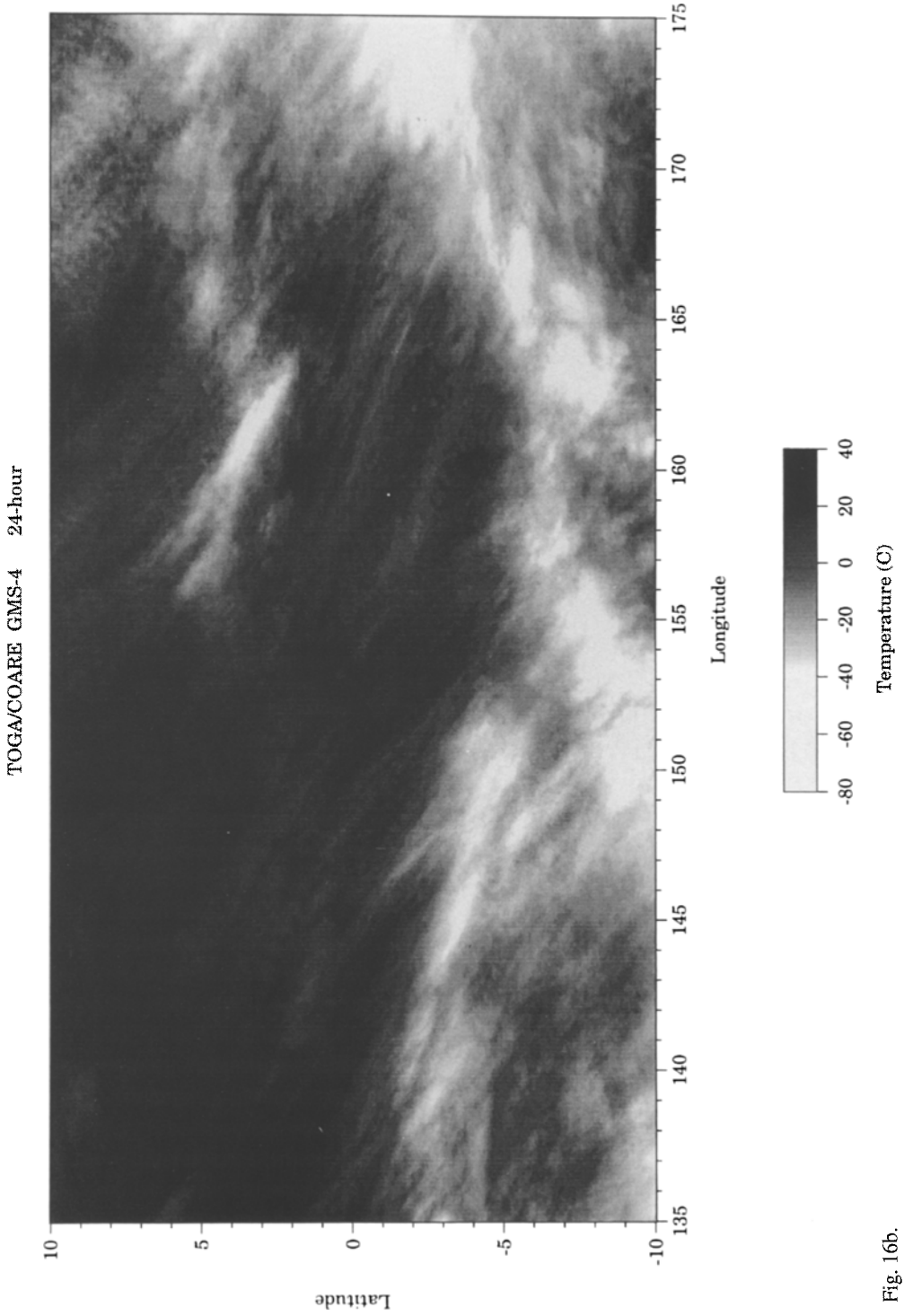
TOGA/COARE GMS-4 24-hour
Latitude
10
5
0
-5
-10
135
140
145
150
155
160
165
170
175
Longitude
-80
-60
-40
-20
0
20
40
Temperature (C)

Fig. 16b.

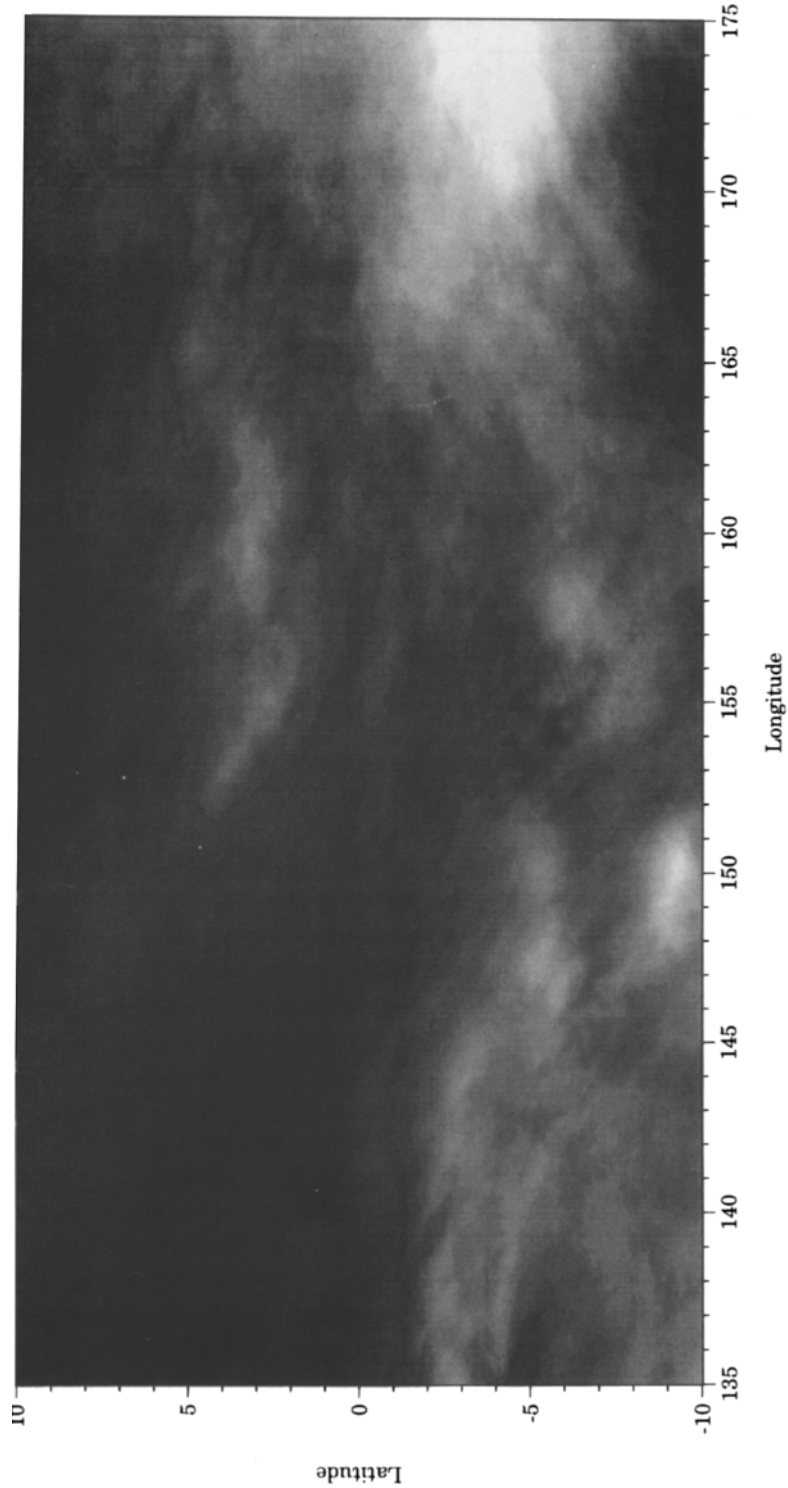

Fig. 16c.

Fig. 16(a)–(c). Grey scale representation of infrared brightness temperature images from the Japanese GMS-4 satellite for the western equatorial Pacific (TOGA-COARE) region at a spatial resolution of 5 km (Flament and Bernstein, 1993): (a) single image; (b) average of 24 images; and (c) average of 240 images.

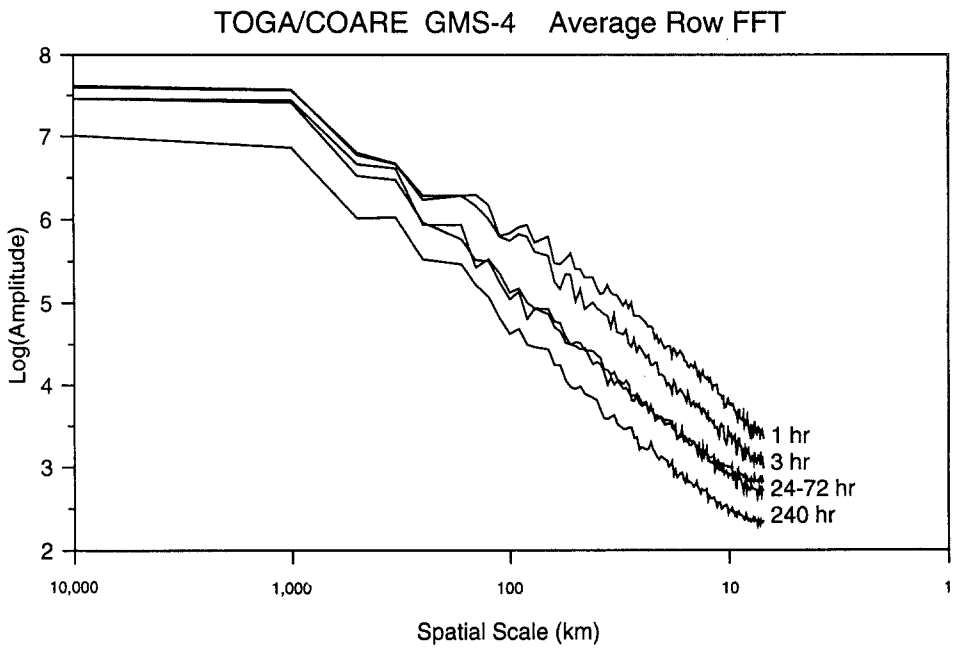

Fig. 17. Spatial power spectra of the infrared brightness temperatures for longitudinal strips through the western equatorial Pacific region shown in Figure 16 (averaged over all latitudinal bands to reduce variance of the spectral estimate). The spatial spectra are evaluated after the brightness temperatures have been averaged over the time intervals indicated: 1 hour (single image), 3 hours, 24 hours, 72 hours and 240 hours.

which covers about 80% of the globe by assuming that each observation represents rather large areas ($\sim$ 1000 km across). If we compare months that have nearly identical original average cloud amounts (within 0.5%), the range of average cloud amounts produced from the partial dataset is almost three times larger. In other words, the apparent cloud amount variation is almost three times 'noisier' than it actually is. Hence, diagnostic monitoring of clouds requires globally complete observations that are only feasible from satellites.

The sampling of clouds required to detect changes must also be 'dense' enough to acquire proper statistics for the significant time and space scales of cloud variation. In the previous section we have shown that the smallest variation time scale that persists in the long-term statistics is the diurnal scale (actually the semi-diurnal scale – Figure 12), whereas most of the variation at spatial scales < 500 km is eliminated in long-term averages (Figure 17). Thus, cloud observations must provide an unbiased sample of the diurnal cycle, but only need a sufficiently small spatial sampling interval to get enough samples of the smaller spatial scale variations.

Global coverage and diurnal sampling cannot be accomplished with observations from one satellite (Salby, 1982); hence, the minimum satellite observing system for cloud monitoring is two satellites (Figure 19) (Brooks *et al.*, 1986; McConnell and North, 1987; Shin and North, 1988; Bell *et al.*, 1990). One satellite

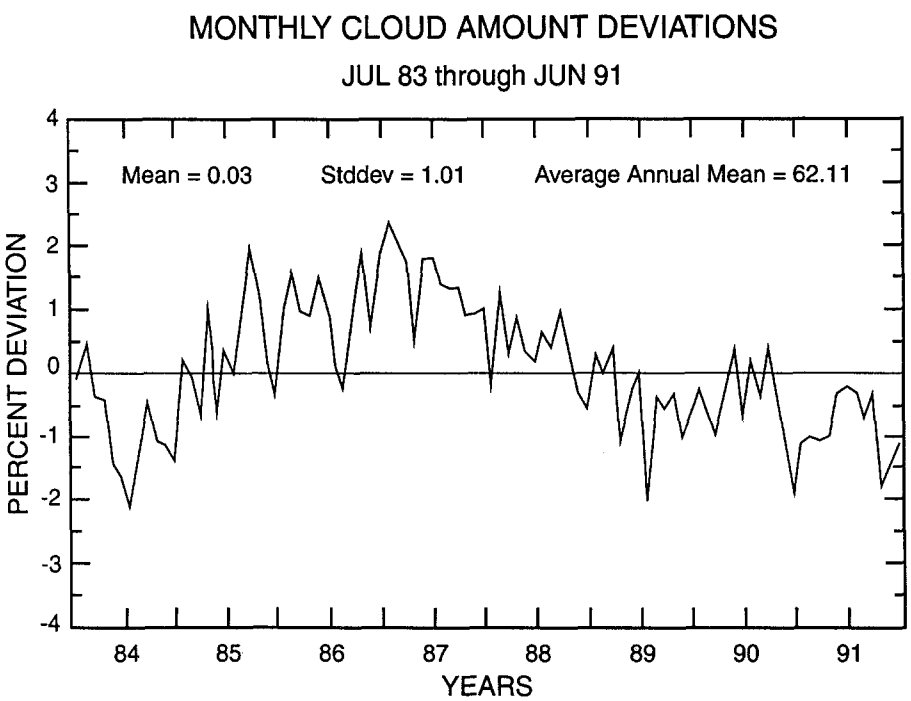

Fig. 18. Variation of the globally averaged, monthly mean cloud amount deviation from the average over the period July 1983 through June 1991 from the ISCCP dataset.

provides global coverage at two times of day and one satellite provides statistical coverage of the diurnal variations at lower latitudes. This minimum system is sufficient to produce accurate averages, including an accurate average diurnal cycle; however, this system is not sufficient for diagnosis of the effects of cloud changes because it cannot describe possible changes in the diurnal variation of clouds. Although an **average** diurnal cycle can be obtained statistically, its accurcay depends on an assumption that the diurnal cycle has not changed over some time period. Hence, the diagnostic requirement demands a satellite system that actually resolves the diurnal time scale, which can be done with three, properly separated, sun-synchronous polar orbiters (Figure 19). Similarly although sampling along the satellite nadir track is sufficient for monitoring changes in global mean cloud properties (Hansen *et al.*, 1993), in order to detect possible shifts in storm tracks or near-coastal cloudiness, observations from scanning instruments are preferable.

To test various cloud observing strategies, we simulated the observations of two satellites with the orbits like those illustrated in Figure 19 (upper panel) by sampling the full ISCCP cloud dataset that has an effective resolution of 30 km and 3 hr. The ISCCP dataset is, itself, a sample of satellite observations with an original spatial resolution of about 5 km; but this sample has been shown to capture the statistics of the original 5 km data (Seze and Rossow, 1991a, b). For this test, we collect 6–9

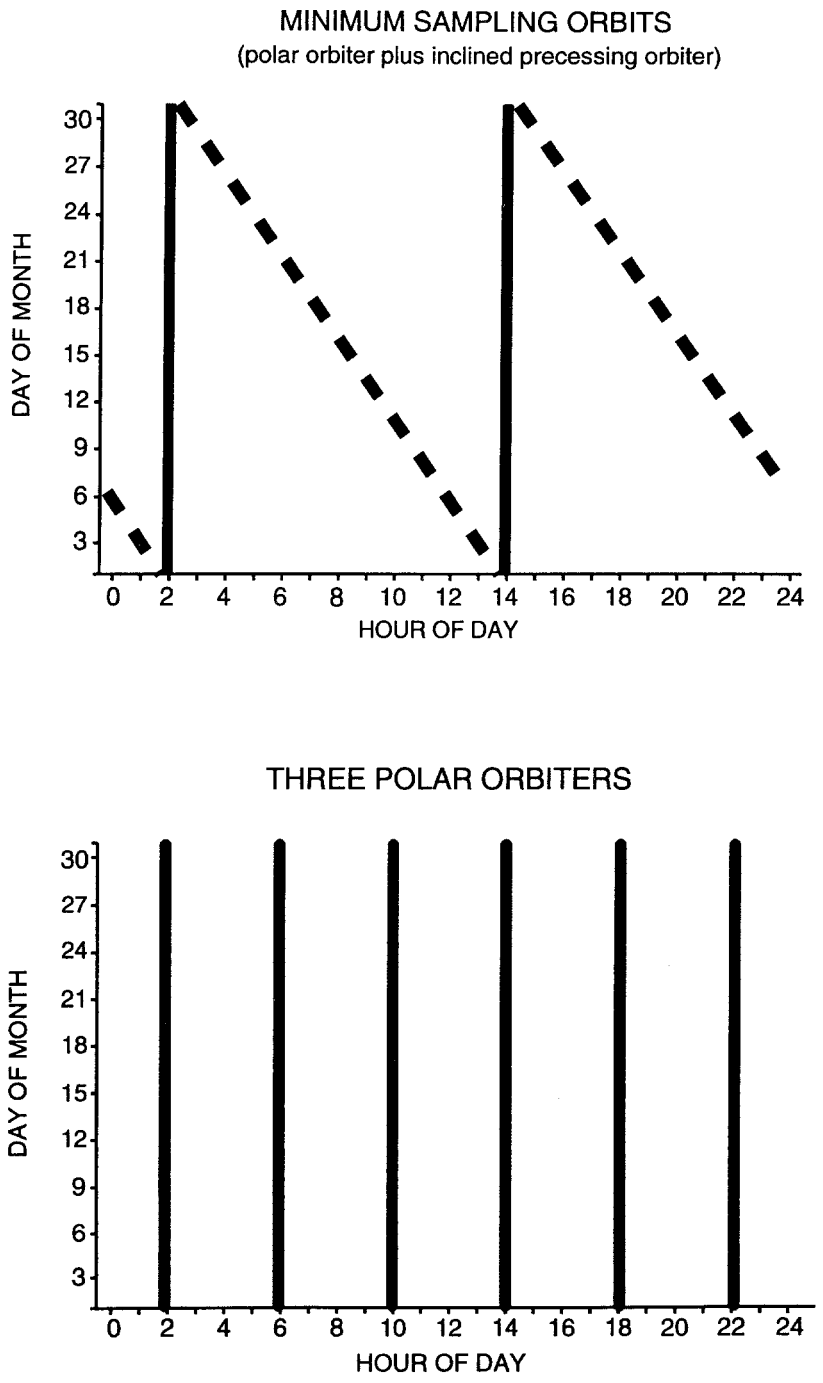

Fig. 19. Two alternative satellite sampling strategies for adequate diurnal sampling illustrated by showing the coverage of time-of-day for each day of the month. The upper panel shows the sampling from one sun-synchronous polar orbiter and an inclined orbiter that drifts in diurnal phase during the month, while the lower panel shows the sampling from three sun-synchronous polar orbiters.

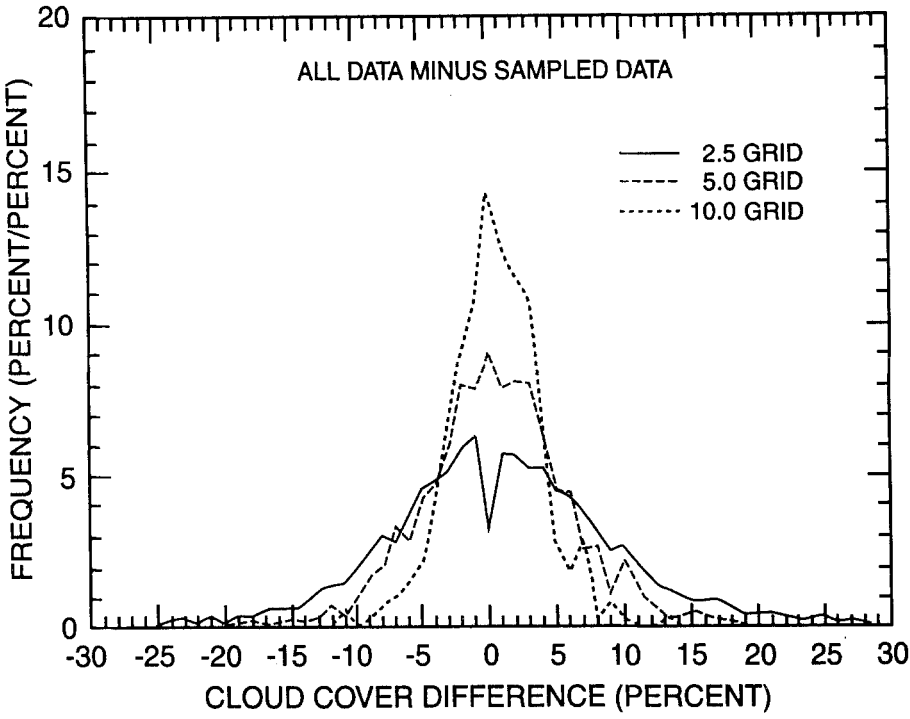

Fig. 20. Frequency distribution over the whole globe of the differences in the regional monthly mean cloud amounts produced from the combined nadir samples of a polar orbiter and an inclined orbiter compared with the full ISCCP sampling. Both datasets are averaged at three different map grid resolutions: 2.5° (solid line), 5.0° (dashed line) and 10° (dotted line).

pixels at each location along the satellite ground track to represent nadir sampling from two satellite orbits. Since we only select a subset of the ISCCP pixels, there is no measurement error, only sampling error in the comparison of the sampled and original data. We focus on cloud cover because its bi-modal frequency distribution (Figure 2) implies a very large natural variability ($\approx$ 30–40%) that produces large sampling effects. The frequency distribution can be thought of as a probability distribution for a single sample (Warren *et al.*, 1986, 1988), so that more than 1000 samples are required to reduce sampling uncertainty below 1%.

To evaluate the accuracy of the sampled dataset, we first calculate the monthly mean cloud cover for each region on Earth on three map grids: 2.5°, 5° and 10°. This is done for the full ISCCP and sampled datasets. We also calculate these averages over three months (one season). The mapped values from the sampled dataset are compared with the full ISCCP values (considered to be the truth) and the frequency distribution of the differences collected. Figure 20 shows these difference distributions for one month averages. Enlarging the averaging domain from 2.5° to 10° decreases the standard deviation of the differences from $\approx$ 8% to $\approx$ 3% and averaging over three months (not shown) decreases the standard deviations from $\approx$ 8% to $\approx$ 5% for the 2.5° map grid and from $\approx$ 3% to $\approx$ 2% for the 10° map grid.

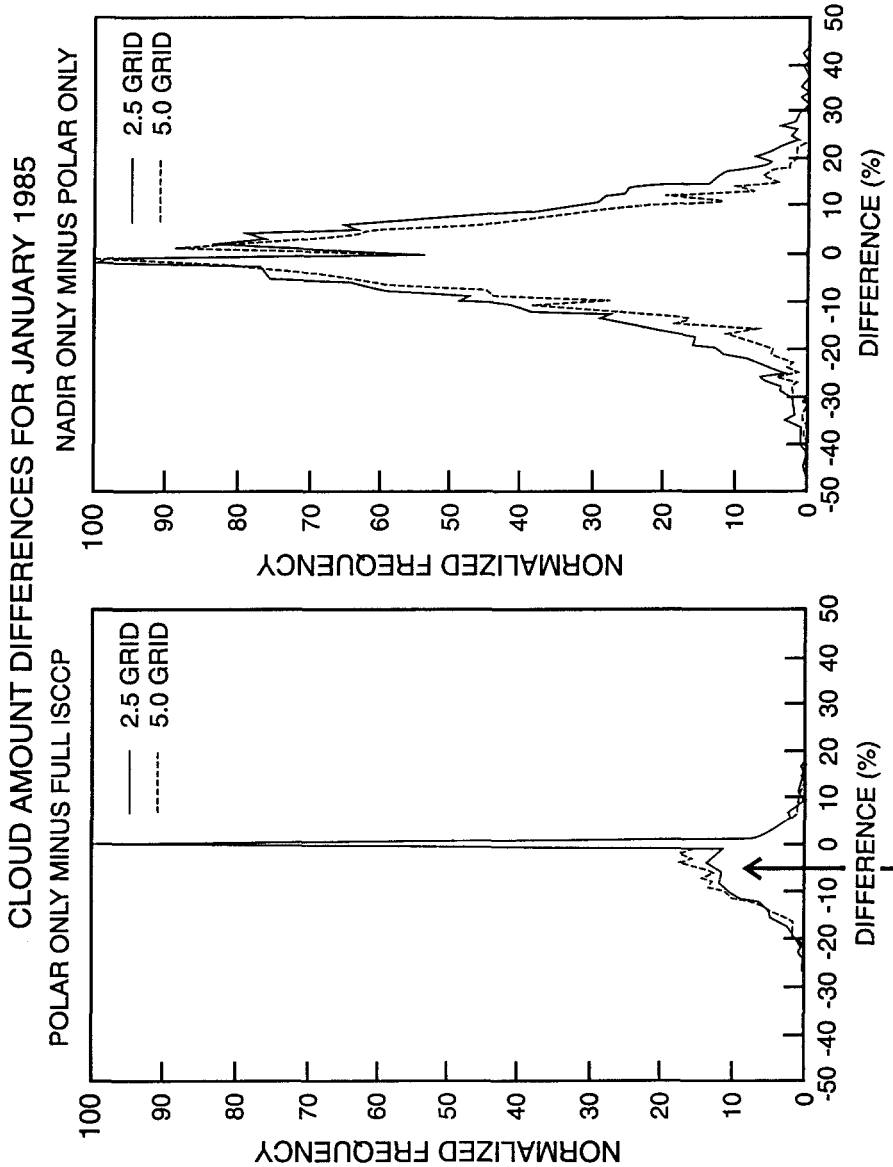

Fig. 21. Frequency distribution over the whole globe of the differences in the regional monthly mean cloud amounts produced from a single polar orbiter compared with the full ISCCP sampling (left panel). The right panel shows the differences between the full and sampled polar orbiter cloud amounts. Results are shown for two map grid resolutions, 2.5° (solid lines) and 5.0° (dashed lines).

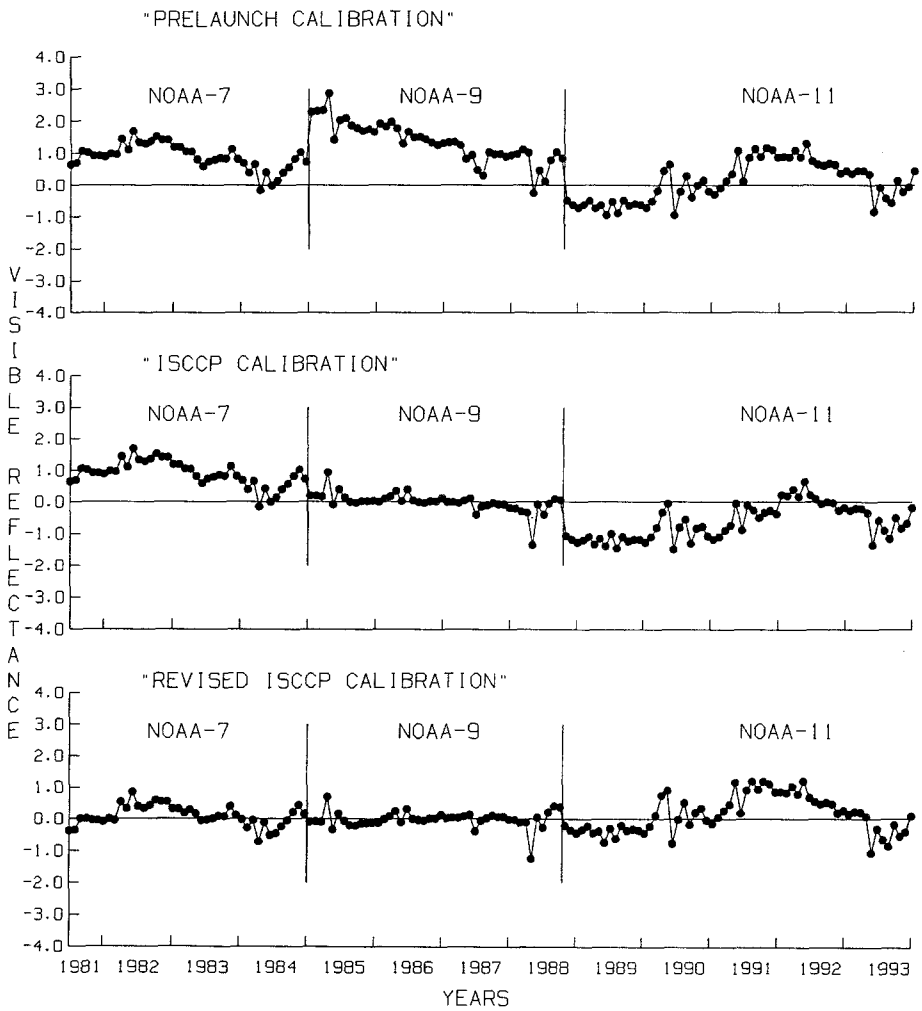

Fig. 22. Variation of the globally averaged, surface visible reflectances over the period July 1983 through December 1993 as deviations from the average values over the NOAA-9 results in the middle panel. The upper panel shows the prelaunch calibration for NOAA-7, NOAA-9 and NOAA-11 and next two panels show the results of two analyses to remove the calibration discontinuities. The remaining anomaly in 1991–1992 is caused by the Pinatubo volcanic aerosol.

The bias error in the global mean cloud amount is < 0.5% for all cases. Thus, the sampling error by the minimum (two-satellite) observing system would just allow measurement of the cloud amount changes shown in Figure 18.

The bias error introduced by incomplete diurnal sampling is illustrated by comparing the results obtained only from the sun-synchronous polar orbiter (samples roughly at 0230 and 1430 local time) with the full ISCCP results (cf. Salby, 1988b; Bell *et al.*, 1990); Figure 21 shows the distribution of differences in monthly mean cloud amounts. Although the global mean bias is not too large, the shape of the

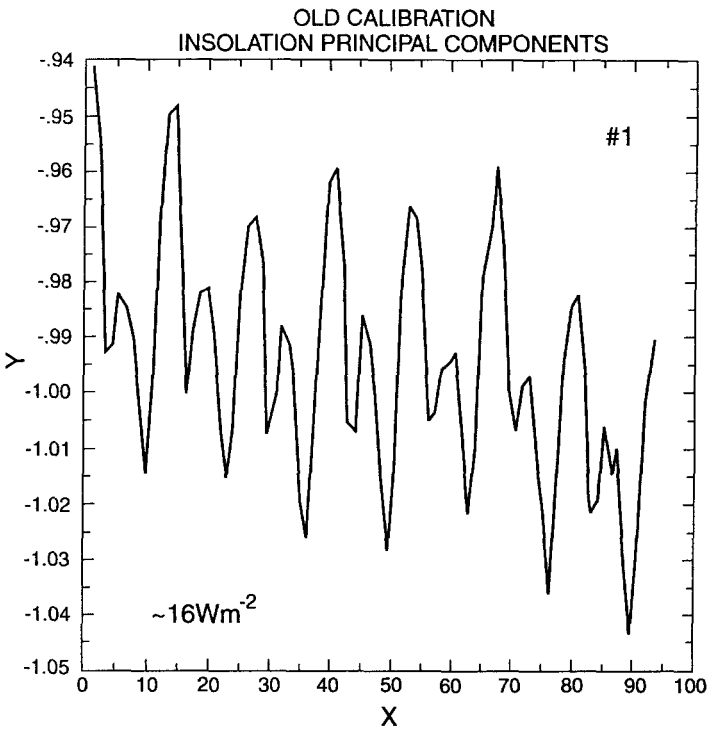

Fig. 23a.

difference histogram clearly shows that biases are much larger in some regions where the amplitude of the diurnal cycle is larger.

5. Calibration

Since small changes in the physical properties of clouds can produce important changes in the radiation balance, a cloud monitoring system must also maintain a uniform relative calibration over the whole data record. For example, to detect changes of cloud top pressure of 10 mb requires a relative calibration accuracy of satellite-measured IR radiances of about 0.2% ($\approx$ 0.5 K in brightness temperature); to detect a change of cloud optical thickness of 0.15 requires a relative calibration accuracy of visible radiances of about 1%. To monitor changes in cloud types requires that the calibration be maintained consistently over all wavelengths used. With today's satellite instruments, these relative accuracies are not attainable from *independent* information. Figure 22 shows three versions of the visible radiance calibration for the ISCCP dataset; only the 'pre-launch' calibration is independent information. The remaining two calibrations use the time record of observations of Earth's surface reflectance to remove differences between different radiometers in the series and to remove sensor sensitivity changes. Note, however, that this

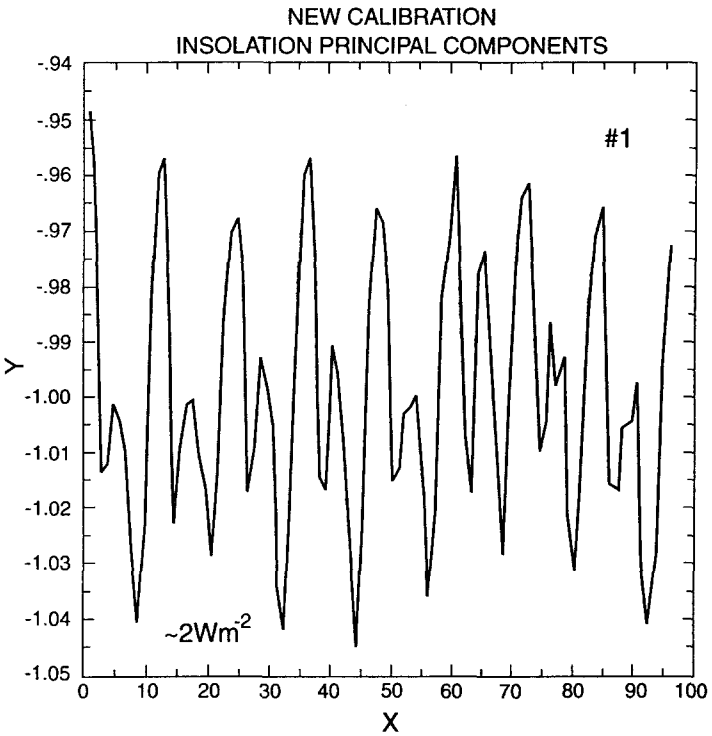

Fig. 23b.

Figs. 23(a)–(b). Time series associated with the first principal components of monthly mean surface solar insolation calculated from ISCCP cloud properties with: (a) the initial ISCCP calibration (second panel in Figure 22); and (b) the revised ISCCP calibration (third panel in Figure 22). The magnitude of the trend in (a) is about 16 Wm^{-2} and in (b) no more than 2 Wm^{-2}. The x-axis represents a time period of eight years, July 1983–June 1991.

procedure must assume that *Earth is, on average, a constant radiometric target*, hence, there is no independent determination as to whether this is actually the case. Figure 23a shows the first principal component of the monthly mean surface solar insolation determined from the ISCCP cloud properties derived with the second calibration. The presence of two small residual (< 10%) discontinuities in the second calibration produces a spurious trend in the surface insolation record with an overall variation of about 16 Wm^{-2} ($\approx$ 8% of the global annual mean value). Removal of these two discontinuities in the third calibration also removes the trend (to within 2 Wm^{-2}) in the surface insolation record (Figure 23b). The current ISCCP results exhibit an apparent decreasing trend in cloud optical thickness and cloud top temperature, most of which appears to be associated with the calibration discontinuities (Klein and Hartmann, 1993).

6. Necessary Attributes of Cloud Monitoring System

Based on this review and assessment of the characteristics of cloud variations, we can briefly outline some of the **necessary** attributes of a cloud monitoring system.

1. complete global coverage with uniform density;
2. spatial sampling interval $\leq$ 50 km;
3. sampling frequency $\geq$ 6 times per day;
4. record length > 10 years with uniform density.

To maintain uniform instrument calibration to the needed very high precision ($\approx$ 1%), overlapping observations between each pair of instruments in the series are essential. Moreover, if actual climate changes are to be detected, calibration must be obtained from information independent of the climate.

References

Barrett, E. C. and Grant, C. L.: 1979, 'Relations between Frequency Distributions of Cloud over the United Kingdom Based on Conventional Observations and Imagery from LANDSAT 2', *Weather* **34**, 416–424.

Bell, T. L.: 1987, 'A Space-Time Stochastic Model of Rainfall for Satellite Remote-Sensing Studies', *J. Geophys. Res.* **92**, 9631–9643.

Bell, T. L., Abdullah, A., Martin, R. L., and North, G. R.: 1990, 'Sampling Errors for Satellite-Derived Tropical Rainfall: Monte Carlo Study Using a Space-Time Stochastic Model', *J. Geophys. Res.* **95**, 2195–2206.

Brest, C. L. and Rossow, W. B.: 1992, 'Radiometric Calibration and Monitoring of NOAA AVHRR Data for ISCCP', *Int. J. Remote Sensing* **13**, 235–273.

Brooks, D. R., Harrison, E. F., Minnis, P., Suttles, J. T., and Kandel, R. S.: 1986, 'Development of Algorithms for Understanding the Temporal and Spatial Variability of the Earth's Radiation Balance', *Rev. Geophys.* **24**, 422–438.

Cahalan, R. F. and Joseph, J. H.: 1982, 'Fractal Statistics of Cloud Fields', *Mon. Wea. Rev.* **117**, 261–272.

Cahalan, R. F., Ridgeway, W., Wiscombe, W. J., Bell, T. L., and Snider, J. B.: 1994, 'The Albedo of Fractal Stratocumulus Clouds', *J. Atmos. Sci.* **51**, 2434–2455.

Cairns, B.: 1995, 'Diurnal Variations of Cloud from ISCCP Data', *Atmos. Res.* **37**, 133–146.

Carlson, B. E., Cairns, B., and Rossow, W. B.: 1995, 'Spatial and Temporal Characterization of Diurnal Cloud Variability Using ISCCP', *J. Clim.*, (submitted).

Cox, S. K., McDougal, D. S., Randall, D. A., and Schiffer, R. A.: 1987, 'FIRE – the First ISCCP Regional Experiment', *Bull. Amer. Meteor. Soc.* **68**, 114–118.

Elliott, W. P. and Gaffen, D. J.: 1991, 'On the Utility of Radiosonde Humidity Archives for Climate Studies', *Bull. Amer. Meteor. Soc.* **72**, 1507–1520.

Flament, P. and Bernstein, R.: 1993, *Images from the GMS-4 Satellite During TOGA-COARE (November 1992 to February 1993)*, Tech. Rep. 93–06, School of Ocean and Earth Sciences and Technoloy, Univ. Hawaii, Honolulu, 20 pp. with two CDROMs.

Fu, R., Del Genio, A. D., and Rossow, W. B.: 1990, 'Behavior of Deep Convective Clouds in the Tropical Pacific Deduced from ISCCP Radiance Data', *J. Clim.* **3**, 1129–1152.

Gaffen, D. J., Barnett, T. P., and Elliott, W. P.: 1991, 'Space and Time Scales of Global Tropospheric Moisture', *J. Clim.* **4**, 989–1008.

Gaster, M. and Roberts, J. B.: 1977, 'The Spectral Analysis of Randomly Sampled Record by a Direct Transform', *Proc. R. Soc. Lond. A.* **354**, 27–58.

Hahn, C. J., Warren, S. G., and London, J.: 1994, *Edited Synoptic Cloud Reports from Ships and Land Stations over the Globe, 1982–1991*, Carbon Dioxide Information Analysis Center, Oak Ridge National Laboratory, Oak Ridge, Tennessee, 47 pp.

Hansen, J. E. and Lebedeff, S.: 1988, 'Global Trends of Measured Surface Air Temperature', *J. Geophys. Res.* **92**, 13, 345–372.

Hansen, J., Rossow, W., and Fung, I.: 1993, *Long-Term Monitoring of Global Climate Forcings and Feedbacks*, NASA Conference Publication 3234, 89 pp.

Harshvardhan, Wielicki, B. A., and Ginger, K. M.: 1994, 'The Interpretation of Remotely Sensed Cloud Properties from a Model Parameterization Perspective', *J. Clim.* **7**, 1987–1998.

Hendon, H. H. and Woodbury, K.: 1993, 'The Diurnal Cycle of Tropical Convection', *J. Geophys. Res.* **98**, 16, 623–16, 637.

Houze, R. A., Rutledge, S. A., Bifferstaff, M. I., and Smull, B. F.: 1989, 'Interpretation of Doppler Weather Radar Displays of Midlatitude Mesoscale Convective Systems', *Bull. Amer. Meteor. Soc.* **70**, 608–619.

Joseph, J. H. and Cahalan, R. H.: 1990, 'Nearest Neighbor Spacing of Fair Weather Cumulus Clouds', *J. Appl. Meteor.* **29**, 793–805.

Kaimal, J., Wyngaard, J. C., Haugen, D. A., Cote, O. R., Izumi, Y., Caughey, S. J., and Readings, C. J.: 1976, 'Turbulence Structure in the Convective Boundary Layer', *J. Atmos. Sci.* **33**, 2152–2169.

Klein, S. A. and Hartmann, D. L.: 1993, 'Spurious Trends in the ISCCP C2 Dataset', *Geophys. Res. Lett.* **20**, 455–458.

Kondragunta, C. R. and Gruber, A.: 1994, 'Diurnal Variations of the ISCCP Cloudiness', *Geophys. Res. Lett.* **21**, 2015–2018.

Kropfli, R. A., Matrosov, S. Y., Uttal, T., Orr, B. W., Frisch, A. S., Clark, K. A., Bartram, B. W., Reinking, R. F., Snider, J. B., and Martner, B. E.: 1995, 'Studies of Cloud Microphysics with Millimeter Wave Radar', *Atmos. Res.* **35**, 299–313.

Kuo, K. S., Welch, R. M., and Sengupta, S. K.: 1988, 'Structural and Textural Characteristics of Cirrus Clouds Observed Using High Spatial Resolution LANDSAT Imagery', *J. Appl. Meteor.* **27**, 1242–1260.

Lau, N.-C. and Crane, M. W.: 1995, 'A Satellite View of the Synoptic-Scale Organization of Cloud Properties in Midlatitude and Tropical Circulation Systems', *Mon. Wea. Rev.* **123**, 1984–2006.

Lee, J., Chou, J., Weger, R. C., and Welch, R. M.: 1994, 'Clustering, Randomness, and Regularity in Cloud Fields, 4, Stratocumulus Cloud Fields', *J. Geophys. Res.* **99**, 14, 461–480.

Liao, X., Rossow, W. B., and Rind, D.: 1995a, 'Comparison between SAGE II and ISCCP High-Level Clouds, Part I: Global and Zonal Mean Cloud Amounts', *J. Geophys. Res.* **100**, 1121–1135.

Liao, X., Rossow, W. B., and Rind, D.: 1995b, 'Comparison between SAGE II and ISCCP High-Level Clouds, Part II: Locating Cloud Tops', *J. Geophys. Res.* **100**, 1137–1147.

Lin, B. and Rossow, W. B.: 1994, 'Observation of Cloud Liquid Water Path over Oceans: Optical and Microwave Remote Sensing Methods', *J. Geophys. Res.* **99**, 20, 907–20, 927.

Machado, L. A. T., Desbois, M., and Duvel, J-P.: 1992, 'Structural Characteristics of Deep Convective Systems over Tropical Africa and Atlantic Ocean', *Mon. Wea. Rev.* **120**, 392–406.

Machado, L. A. T., Duvel, J-P., and Desbois, M.: 1993, 'Diurnal Variations and Modulation by Easterly Waves of the Size Distribution of Convective Cloud Clusters over West Africa and the Atlantic Ocean', *Mon. Wea. Rev.* **121**, 37–49.

Machado, L. A. T. and Rossow, W. B.: 1993, 'Structural Characteristics and Radiative Properties of Tropical Cloud Clusters', *Mon. Wea. Rev.* **121**, 3234–3260.

McConnell, A. and North, G. R.: 1987, 'Sampling Errors in Satellite Estimates of Tropical Rain', *J. Geophys. Res.* **92**, 9567–9570.

Mokhov, I. I. and Schlesinger, M. E.: 1993, 'Analysis of Global Cloudiness, 1, Comparison of ISCCP, Meteor and Nimbus 7 Satellite Data', *J. Geophys. Res.* **98**, 12, 849–12, 868.

Mokhov, I. I. and Schlesinger, M. E.: 1994, 'Analysis of Global Cloudiness, 2, Comparison of Ground-Based and Satellite-Based Cloud Climatologies', *J. Geophys. Res.* **99**, 17, 045–17, 065.

Nicholls, S.: 1989, 'The Structure of Radiatively Driven Convection in Stratocumulus', *Quart. J. Roy. Meteorol. Soc.* **115**, 487–511.

Pandolfo, L.: 1993, 'Observational Aspects of the Low-Frequency Intraseasonal Variability of the Atmosphere in Middle Latitudes', *Adv. Geophys.* **34**, 93–174.

Parker, L., Welch, R. M., and Musil, D. J.: 1986, 'Analysis of Spatial Inhomogeneities in Cumulus Clouds Using High Spatial Resolution LANDSAT Data', *J. Clim. Appl. Meteorol.* **25**, 1301–1314.
Priestly, M. B.: 1981, *Spectral Analysis and Time Series*, Academic, New York.
Rossow, W. B.: 1978, 'Cloud Microphysics: Analysis of the Clouds of Earth, Venus, Mars, and Jupiter', *Icarus* **36**, 1–50.
Rossow, W. B.: 1989, 'Measuring Cloud Properties from Space: A Review', *J. Clim.* **2**, 201–213.
Rossow, W. B. and Lacis, A. A.: 1990, 'Global, Seasonal Cloud Variations from Satellite Radiance Measurements. Part II: Cloud Properties and Radiative Effects', *J. Clim.* **3**, 1204–1253.
Rossow, W. B. and Garder, L. C.: 1993a, 'Cloud Detection Using Satellite Measurements of Infrared and Visible Radiances for ISCCP', *J. Clim.* **6**, 2341–2369.
Rossow, W. B. and Garder, L. C.: 1993b, 'Validation of ISCCP Cloud Detections', *J. Clim.* **6**, 2370–2393.
Rossow, W. B. and Schiffer, R. A.: 1991, 'ISCCP Cloud Data Products', *Bull. Amer. Meteor. Soc.* **72**, 2–20.
Rossow, W. B., Walker, A. W., and Garder, L. C.: 1993, 'Comparison of ISCCP and Other Cloud Amounts', *J. Clim.* **6**, 2394–2418.
Rossow, W. B. and Zhang, Y-C.: 1995, 'Calculation of Surface and Top-of Atmosphere Radiative Fluxes from Physical Quantities Based on ISCCP Datasets, Part II: Validation and First Results, *J. Geophys. Res.* **100**, 1167–1197.
Salby, M. L.: 1982, 'Sampling Theory for Asynoptic Satellite Observations. Part I: Space-Time Spectra, Resolution, and Aliasing', *J. Atmos. Sci.* **39**, 2577–2600.
Salby, M. L.: 1988a, 'Asynoptic Sampling Considerations for Wide-Field-of-View Measurements of Outgoing Radiation. Part I: Spatial and Temporal Resolution', *J. Atmos. Sci.* **45**, 1176–1183.
Salby, M. L.: 1988b, 'Asynoptic Sampling Considerations for Wide-Field-of-View Measurements of Outgoing Radiation. Part II: Diurnal and Random Space-Time Variability', *J. Atmos. Sci.* **45**, 1184–1204.
Salby, M. L.: 1989, 'Climate Monitoring from Space: Asynoptic Sampling Considerations', *J. Clim.* **2**, 1091–1105.
Salby, M. L., Hendon, H. H., Woodbury, K., and Tanaka, K.: 1991, 'Analysis of Global Cloud Imagery from Multiple Satellites', *Bull. Amer. Meteor. Soc.* **72**, 467–480.
Sassen, K.: 1991, 'The Polarization Lidar Technique for Cloud Research: A Review and Current Assessment', *Bull. Amer. Meteor. Soc.* **72**, 1848–1866.
Sengupta, S. K., Welch, R. M., Navar, M. S., Berendes, T. A., and Chen, D. W.: 1990, 'Cumulus Cloud Field Morphology and Spatial Patterns Derived from High Spatial Resolution LANDSAT Imagery', *J. Appl. Meteor.* **29**, 1245–1267.
Seze, G. and Rossow, W. B.: 1991a, 'Time-Cumulated Visible and Infrared Radiance Histograms Used as Descriptors of Surface and Cloud Variations', *Int. J. Remote Sensing* **12**, 877–920.
Seze, G. and Rossow, W. B.: 1991b, 'Effects of Satellite Data Resolution on Measuring the Space-Time Variations of Surfaces and Clouds', *Int. J. Remote Sensing* **12**, 921–952.
Shapiro, H. S. and Silverman, R. A.: 1960, 'Alias-Free Sampling of Random Noise', *J. SIAM* **8**, 225–248.
Shin, K.-S. and North, G. R.: 1988, 'Sampling Error Study for Rainfall Estimate by Satellite Using Stochastic Model', *J. Appl. Meteor.* **27**, 1218–1231.
Stowe, L. L., Wellemeyer, C. G., Eck, T. F., Yeh, H. Y. M. and the NIMBUS-7 Cloud Data Processing Team: 1988, 'NIMBUS-7 Global Cloud Climatology. Part I: Algorithms and Validation', *J. Clim.* **1**, 445–470.
Stowe, L. L., Yeh, H. Y. M., Eck, F. T., Wellemeyer, C. G., Kyle, H. L. and the NIMBUS-7 Cloud Data Processing Team: 1989, 'NIMBUS-7 Global Cloud Climatology. Part II: First Year Results', *J. Clim.* **2**, 671–709.
Thomson, D. J.: 1990, 'Quadratic-Inverse Spectrum Estimates: Application to Paleoclimatology', *Phil. Trans. Roy. Soc. Lond.* **A332**, 539–597.
Wang, J. and Rossow, W. B.: 1995, 'Determination of Cloud Vertical Structure from Upper Air Observations', *J. Appl. Meteor.*, (in press).
Warren, S. G., Hahn, C. J., and London, J.: 1985, 'Simultaneous Occurrence of Different Cloud Types', *J. Clim. Appl. Meteor.* **24**, 658–667.

Warren, S. G., Hahn, C. J., London, J., Chervin, R. M., and Jenne, R. L.: 1986, *Global Distribution of Total Cloud and Cloud Type Amounts over Land*, 29 pp. + 200 maps, (NTIS number DE87–00–6903).

Warren, S. G., Hahn, C. J., London, J., Chervin, R. M., and Jenne, R. L.: 1988, *Global Distribution of Total Cloud and Cloud Type Amounts over the Ocean*, 42 pp. + 170 maps, (NTIS number DE90–00–3187).

Weger, R. C., Lee, J., Zhu, T., and Welch, R. M.: 1992, 'Clustering, Randomness, and Regularity in Cloud Fields, 1, Theoretical Considerations', *J. Geophys. Res.* **97**, 20, 519–20, 536.

Weger, R. C., Lee, J., and Welch, R. M.: 1993, 'Clustering, Randomness, and Regularity in Cloud Fields, 3, The Nature and Distribution of Clusters', *J. Geophys. Res.* **98**, 18, 449–18, 463.

Welch, R. M., Kuo, K. S., Wielicki, B. A., Sengupta, S. K., and Parker, L.: 1988, 'Marine Stratocumulus Cloud Fields off the Coast of Southern California Observed Using LANDSAT Imagery. Part I: Structural Characteristics', *J. Appl. Meteor.* **27**, 341–362.

Wielicki, B. A. and Parker, L.: 1992, 'On the Determination of Cloud Cover from Satellite Sensors: The Effects of Sensor Spatial Resolution', *J. Geophys. Res.* **97**, 12, 799–12, 823.

Wielicki, B. A. and Welch, R. M.: 1986, 'Cumulus Cloud Field Properties Derived Using LANDSAT Digital Data', *J. Clim. Appl. Meteor.* **25**, 261–276.

Zangvil, A.: 1975, 'Temporal and Spatial Behavior of Large-Scale Disturbances in Tropical Cloudiness Deduced from Satellite Brightness Data', *Mon. Wea. Rev.* **103**, 904–920.

Zhang, Y.-C., Rossow, W. B., Lacis, A. A.: 1995, 'Calculation of Surface and Top-of-Atmosphere Radiative Fluxes from Physical Quantities Based on ISCCP Datasets, Part I: Method and Sensitivity to Input Data Uncertainties', *J. Geophys. Res.* **100**, 1149–1165.

Zhu, T., Lee, J., Weger, R. C., and Welch, R. M.: 1992, 'Clustering, Randomness, and Regularity in Cloud Fields, 2, Cumulus Cloud Fields', *J. Geophys. Res.* **97**, 20, 537–20, 558.

(Received 23 January, 1995; in revised form 17 July, 1995)